

A POTENTIAL LONG-LIVED UPPER CRETACEOUS PALEODRAINAGE SYSTEM IN
THE U.S. SOUTHWESTERN GEORGIA-SOUTHEASTERN ALABAMA REGION

Daniel Lamar Black

A POTENTIAL LONG-LIVED UPPER CRETACEOUS PALEODRAINAGE SYSTEM IN
THE U.S. SOUTHWESTERN GEORGIA-SOUTHEASTERN ALABAMA REGION

A POTENTIAL LONG-LIVED UPPER CRETACEOUS PALEODRAINAGE SYSTEM IN
THE U.S. SOUTHWESTERN GEORGIA-SOUTHEASTERN ALABAMA REGION

A thesis submitted to the College of Letters and Science in partial fulfillment of the requirements
for the degree of

MASTER OF SCIENCE

DEPARTMENT OF EARTH AND SPACE SCIENCE

by

Daniel L. Black

2015

Clinton Barineau

4-17-2015

Dr. Clinton Barineau, Chair

William Frazier

Dr. William Frazier, Member

Roger W Brown

Dr. Roger Brown, Member

4/17/15

Date

William Frazier

Dr. William Frazier, Department Chair

COLUMBUS STATE UNIVERSITY

A POTENTIAL LONG-LIVED UPPER CRETACEOUS PALEODRAINAGE SYSTEM IN
THE U.S. SOUTHWESTERN GEORGIA-SOUTHEASTERN ALABAMA REGION

A THESIS SUBMITTED TO
THE COLLEGE OF LETTERS AND SCIENCES
IN PARTIAL FULFILLMENT OF
THE REQUIREMENTS FOR THE DEGREE OF

MASTER OF SCIENCE
DEPARTMENT OF EARTH AND SPACE SCIENCES

BY
DANIEL L. BLACK

COLUMBUS, GEORGIA

2015

A POTENTIAL SOURCE-LEAD LAYER OF THE FAIRFAX PALEOGLACIATION SYSTEM IN
THE U.S. SOUTHWESTERN GLACIERS-YOUTHFUL ALABAMA RAILWAY

Copyright © 2015 Daniel L. Black

All Rights Reserved.

Second Page Approved:

Christopher Clark
Clemson State University
March 2015

A POTENTIAL LONG-LIVED UPPER CRETACEOUS PALEODRAINAGE SYSTEM IN
THE U.S. SOUTHWESTERN GEORGIA-SOUTHEASTERN ALABAMA REGION

from sedimentary rocks of the Coastal Plain. In the Columbus, Georgia region, tectonic rocks
of the Higher Tuscaloosa are typically sandstone, siltstone and gravel of the Tuscaloosa Formation.

Sediments within the Tuscaloosa Formation. By lateral derivation from granite of the
Columbus Metacanthite Complex, or from the Mountain belt and potentially rocks of lower
Tuscaloosa River Ridge area.

Daniel L. Black

Lower Chattahoochee River Valley reflects the presence of one or more large paleovalleys in

The Upper Cretaceous stratigraphic column. Committee Chair:

Dr. Clinton Barineau

Indicate recognition of Tuscaloosa and Lower Chattahoochee River Valley.

Committee Members:

Dr. William Frazier
Dr. Roger Brown

Signature Page Approved:

Committee Chair
Columbus State University
March 2015

Abstract

The Gulf Coastal Plain unconformity separates crystalline basement of the Appalachian core from sedimentary units of the Coastal Plain. In the Columbus, Georgia region, basement rocks of the Uchee terrane are typically overlain by sands and gravels of the Tuscaloosa Formation. Sediments within the Tuscaloosa Formation indicate partial derivation from gneiss of the Columbus Metamorphic Complex, the nearby Pine Mountain belt and potentially rocks of Inner Piedmont-eastern Blue Ridge terranes. Mapping along the Coastal Plain unconformity near the Lower Chattahoochee River Valley indicates the presence of one or more large paleovalleys in the Upper Cretaceous sub-Coastal Plain surface that occupy a similar position to a paleodrainage system identified in the overlying Eutaw Formation. Characteristics of the Eutaw Formation indicate recycling of Tuscaloosa sediments in addition to crystalline basement sources. Collectively, these data indicate the possibility of a long-lived drainage system in the vicinity of the modern Lower Chattahoochee River Valley.

Acknowledgements

I would first like to thank Dr. Tom Hanley for the use of the immense amount of data that he previously collected. His work provided an excellent starting point for this project. I would also like to thank Cheryl Wilkes and Alex Colon for their work in mapping the Fortson Quadrant as part of an EDMAP project funded by the US Geological Society. Many thanks are due to Dr. Bill Frazier for his help in both identifying Tuscaloosa sediments as well as his previous work in identifying, classifying, and mapping sediments of the Coastal Plain. I also owe Dr. Roger Brown thanks for his assistance with providing a large amount of help with ArcGIS. Additionally, I would like to thank Amanda Snow for all of her help with my field work, identifying plants that I shouldn't step on, pulling me out of creeks that I fell into, and her general support and encouragement. Finally, I thank my advisor Dr. Clint Barineau. Without his guidance, advice, and time spent on many, many edits this project would have never been completed.

Photograph courtesy of the author, permission granted by Tom Hanley, USGS, and Roger Brown, USGS.

Figure 3: Generalized trend section of a likely continental margin (modified from Heege and Lee, 2000).

Figure 4: Study area, in Marion and Lee Counties, AL, and Monroe, Harris, Chambers, Lee, Marion and Talladega, Georgia.

Figure 5: Geologic map of Paleozoic and adjacent terranes (Chamberlain et al., 2005).

Figure 6: Clasts within the Tuscaloosa Formation. Left image—locally derived grayish. Right image—locally derived greenish. Images courtesy of Dr. Bill Frazier.

Figure 7: Palaeoenvironment of the Tuscaloosa Formation of eastern AL and western GA, east of the Fall Line paleodivide (adapted from Frazier, 1999).

Figure 8: Selected stations from the Tuscaloosa Formation, Marion, Monroe, AL, and Columbia, GA used for mineralogical provenance study (Heege, 2005). Red lines show modern drainage boundaries. Blue line shows approximate location of the Upper Cretaceous paleodivide in the Fall Line drainage system.

Table of Contents

Acknowledgements.....	v
List of Figures	vi
List of Tables	viii
Introduction.....	1
Methods.....	11
Independent Checks	17
Results.....	39
Conclusions.....	42
Works Cited	45

List of Figures

Figure 1: Map depicting the Coastal Plain unconformity in Alabama and Georgia.....	2
Figure 2: Stratigraphy of the Uchee terrane (Piedmont), Tuscaloosa Formation, and Eutaw Formation units (Coastal Plain).	3
Figure 3: Generalized cross section of a rifted continental margin (modified from Behn and Lin, 2000).	4
Figure 4: Study area in Russell and Lee Counties, AL and Muscogee, Harris, Chattahoochee, Marion and Talbot Counties, GA.....	4
Figure 5: Geologic map of Uchee and adjacent terranes (Steltenpohl et al, 2008).	6
Figure 6: Clasts within the Tuscaloosa Formation. Left image—locally derived pisoliths. Right image—locally derived gneiss pebbles. Images courtesy of Dr. Bill Frazier.....	8
Figure 7: Paleoenvironment of the Eutaw Formation of eastern AL and western GA, east of the Eutaw paleodivide (adapted from Frazier, 1996).	9
Figure 8: Selected stations from the Eutaw Formation between Montgomery, AL and Columbus, GA used for mineralogical provenance study (Osborne, 2013). Red lines show modern drainage boundaries. Blue line shows approximate location of an Upper Cretaceous paleodivide in the Eutaw drainage system.	10

Figure 9: Heavy mineral modes in selected Eutaw Formation localities identifying a potential Upper Cretaceous paleodivide west of the AL-GA state line (adapted from Osborne, 2013; Black et al., 2014)	11
Figure 10: All new and existing data points.	13
Figure 11: Method for interpolating contact elevations.....	14
Figure 12: Collected data points with observed and interpolated contacts.....	14
Figure 13: Observed and interpolated contacts.....	15
Figure 14: Contours (15m interval) on the CPU. Blue arrows show the location of potential paleochannels.....	15
Figure 15: Comparison of Eutaw paleochannel with proposed Tuscaloosa paleochannel (adapted from Frazier, 1996).	16
Figure 16: Potential pitfall of interpolating contact elevations. Red lines depict extremes in the geometry of the unconformity between observed points below (blue circle) and above (yellow circle) the unconformity. The actual unconformity could lie above or below the interpolated (green circle) position of the unconformity.	17
Figure 17: Cluster of interpolated points showing expected elevation consistency. Red lines indicate 3m contour interval. Green boxes are interpolated contacts. Red boxes are observed contacts. Numbers indicate elevations in meters above sea level for each identified point.	19
Figure 18: Contours (15m interval) of elevation data for metamorphic basement rocks-paleosol.	21
Figure 19: Contours (15m interval) of elevation data for Tuscaloosa Formation clastics.....	22
Figure 20: Paleogeographic reconstruction North America immediately prior to deposition of the Tuscaloosa Formation, ca.105 Ma (Blakey, 2013).	23
Figure 21: Analog for Tuscaloosa Formation depositional environment, southeastern Brazil. ...	25
Figure 22: Comparison of elevation changes for the three Brazilian rivers and the eastern-most CPU paleochannel over a constant distance.	25
Figure 23: Comparison of the cross-valley profiles of the three Brazilian rivers over a constant distance equal to the width of the eastern-most paleochannel.	26
Figure 24: Plot of distances between physical locations used in interpolations. Groups of data points can be used for relief comparison to modern analogues.	28

Figure 25: Transects of Rio Mampituba at three locations as the river leaves the highlands and approaches base level.....	29
Figure 26: Plot of 122m transect segments versus total relief for each segment within Brazilian river valleys used as modern analogues for paleochannels responsible for Tuscaloosa transportation and deposition. Average relief is $\pm 1.0\text{m}$ with outliers removed.....	30
Figure 27: Plot of 305m transect segments versus total relief for each segment within Brazilian river valleys used as modern analogues for paleochannels responsible for Tuscaloosa transportation and deposition. Average relief is $\pm 2.0\text{m}$ with outliers removed.....	31
Figure 28: Plot of 442m transect segments versus total relief for each segment within Brazilian river valleys used as modern analogues for paleochannels responsible for Tuscaloosa transportation and deposition. Average relief is $\pm 3.0\text{m}$ with outliers removed.....	32
Figure 29: Plot of 579m transect segments versus total relief for each segment within Brazilian river valleys used as modern analogues for paleochannels responsible for Tuscaloosa transportation and deposition. Average relief is $\pm 3.4\text{m}$ with outliers removed.....	33
Figure 30: Station DB102. Tuscaloosa outcrop in Phenix City, AL showing an overall fining upward sequence (Image courtesy of Dr. Bill Frazier).....	35
Figure 31: Location of samples used for grain size analysis.	36
Figure 32: DB102 Basal Tuscaloosa Formation sediment is dominated by coarse, gravelly sandstone.....	36
Figure 33: DB102 Sediment from the middle of the Tuscaloosa Formation is dominated by medium to fine-grained massive sandstone.	37
Figure 34: DB100 located at observable contact with basement skewed toward larger grains....	38
Figure 35: DB088 located ~11.6 m above the CPU contact skewed toward finer grains.	38
Figure 36: 3D surface of contact surface produced in ArcGIS using available data. Contour interval is 10ft (3m). Vertical exaggeration is 13:1	40
Figure 37: Overlay of the contact surface model in Google Earth compared to freehand contours (red). Black contour interval is 3m. Red contour interval is 15m.....	41

List of Tables

Table 1: Amount of potential error in interpolated values as shown by comparison to relief present in modern analogs. 32

In southeastern Georgia-southeastern Alabama, the Gulf Coastal Plain unconformity (GCP) is the contact (Fig. 1) between deformed and metamorphosed crystalline rocks of the Appalachia Piedmont to the north, as well as paleozoic dolomitic limestone, and overlying unconformable units of the Gulf Coastal Plain to the south (Fig. 2). The term "Gulf Line" is commonly used to describe the faulted zone boundary to many geologists and is derived from the words and title commonly found in groups crossing the boundary, and is developed across the transition from more northern plutonic, metamorphic rocks to low-grade sedimentary rocks. The GCP developed along the passive continental margin of North America following the breakup of Pangea, with deformation localized at the Caledonides and younger Coastal Plain developing above crystalline basement rocks of the Piedmont terrane to southeastern Georgia and southeastern Alabama (Fig. 2). The surface the GCP can be traced from the latitude of New York along the Atlantic coastal plain to southeastern Georgia and southeastern Alabama. In the Chattahoochee River area of the lower piedmont the River Valley (C.R.V.) (Fig. 4), the unconformity is offset by one prominent west-dipping thrust. In addition to a gradual decline in elevation from about 100 m above sea level to 10 m below sea level within the Chattahoochee River extending from the town of Woodstock to just upstream of Roswell, approximately 8 km in Woodruff Riverfront Park, the location of the northernmost basement exposures within the river. South of this location much of the Piedmont is below ground level and marine units. Work by Eargle (1985) indicates the gradient on the contact within the GCP, which is 25–60 miles (39.3–96.5 km - 336.3 miles) southward. In contrast, Martin and Foothills (1975) indicate the gradient on the unconformity to be approximately 33 miles (53.1 km). Coastal Plain rocks thicken to the south of the unconformity and become more marine in nature. Due to its location

Introduction

In the eastern edge of the Fall Line, the Gulf Coastal Plain unconformity (CPU) is

In southwestern Georgia-southeastern Alabama, the Gulf Coastal Plain unconformity (CPU) is the contact (Fig. 1) between deformed and metamorphosed crystalline rocks of the Appalachian Piedmont to the north, as well as paleosols developed on those rocks, and overlying sedimentary units of the Gulf Coastal Plain to the south (Fig. 2). The term “Fall Line” is commonly used to describe the trace of this boundary in map view and is derived from the rapids and falls commonly found on streams crossing this boundary, which develop across the transition from more resistant plutonic-metamorphic rocks to less-resistant sedimentary rocks. The CPU developed along the passive continental margin of North America following the breakup of Pangea, with sedimentary sequences of the Cretaceous and younger Coastal Plain developing above crystalline basement rocks of the Piedmont terranes in southwestern Georgia and southeastern Alabama (Fig. 3). The trace of the CPU can be traced from the latitude of New York along the Eastern Seaboard through southwestern Georgia and southeastern Alabama. In the Columbus, GA area of the Lower Chattahoochee River Valley (LCRV) (Fig. 4), the unconformity is not marked by any prominent topographic feature, but rather by a gradual decline in elevation most noticeable in the series of rapids within the Chattahoochee River extending from the North Highlands Dam southward approximately 4 km to Woodruff Riverfront Park, the location of the southernmost basement exposures within the river. South of this location rocks of the Piedmont lie below Coastal Plain sedimentary units. Work by Eargle (1955) indicates the gradient on this contact within the LCRV averages 55 – 60 ft/mile (290.4 m/km - 316.8 m/km) toward the southeast. In contrast, Marsalis and Friddell (1975) indicate the gradient on the unconformity to be approximately 33 ft/mile (174.2 m/km). Coastal Plain strata thicken to the south of the unconformity and become more marine in nature. Due to its location

at the eastern edge of the Gulf Coastal Province and western edge of the Atlantic Coastal Province, the geomorphology of the LCRV was affected by oceanographic and tectonic processes of both.



Figure 1: Map depicting the Coastal Plain unconformity in Alabama and Georgia.

Eutaw Fm. Santonian-Campanian	Upper unit: Micaceous, carbonaceous, fossiliferous silts, sands, and clays Basal unit: Course-grained, feldspathic quartzose sand (Marsalis and Friddell, 1975).
<i>Disconformity</i>	
Tuscaloosa Fm. Cenomanian-Santonian	Poorly sorted, coarse grained, sub-angular sands in a kaolin matrix (Marsalis and Friddell, 1975).
<i>Coastal Plain unconformity</i>	
Uchee Terrane Neoproterozoic-Paleozoic	Paleosol: Formed at base of Tuscaloosa. Characterized by bioturbation, iron oxide nodules, and mottled red-orange coloration.
Columbus Metamorphic Complex: Migmatite, orthogneiss, and amphibolite Moffits Mill Schist: Interlayered biotite epidote muscovite quartz schist, metagraywacke, and quartzite Phenix City Gneiss: biotite hornblende gneiss-amphibolite	

Figure 2: Stratigraphy of the Uchee terrane (Piedmont), Tuscaloosa Formation, and Eutaw Formation units (Coastal Plain).

Figure 4: Study area in Russell and Lee Counties, AL, and Monroe, Hamil, Chattooga, Marion and Talbot Counties, GA.

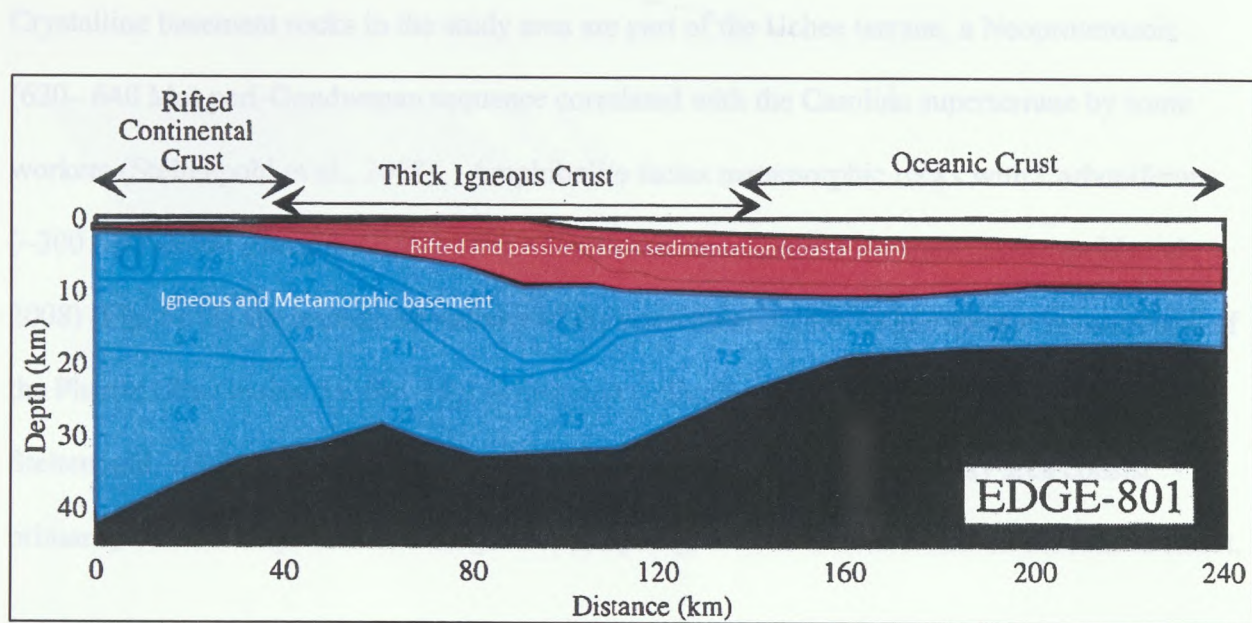


Figure 3: Generalized cross section of a rifted continental margin (modified from Behn and Lin, 2000).

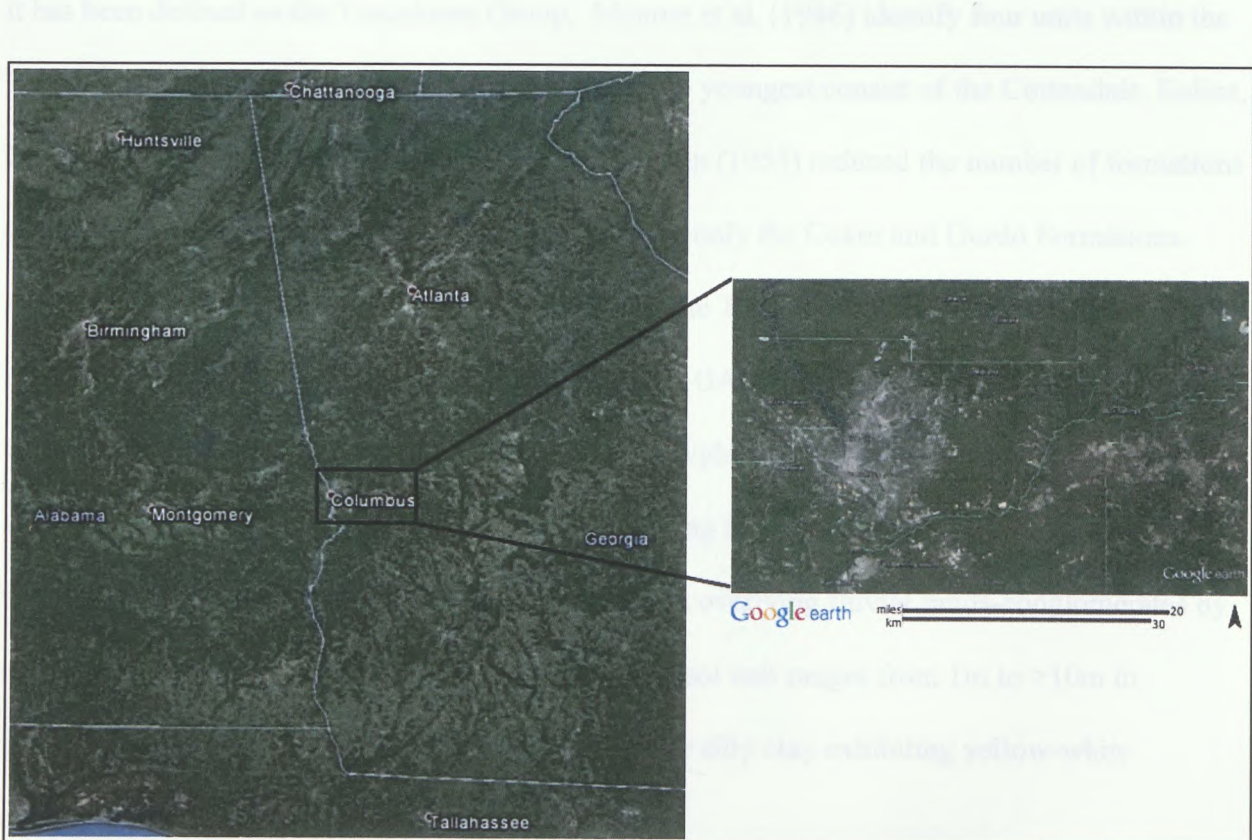


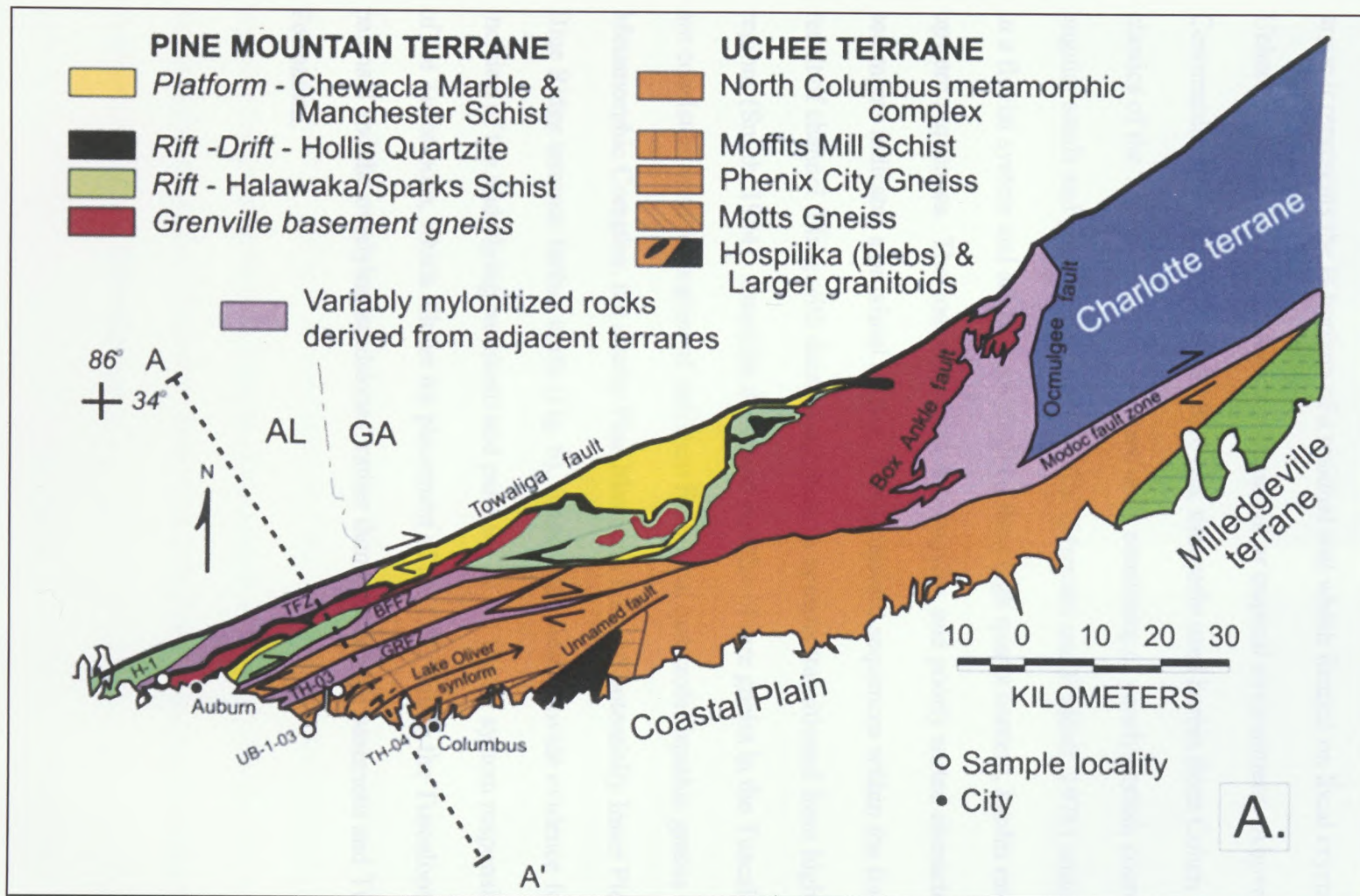
Figure 4: Study area in Russell and Lee Counties, AL and Muscogee, Harris, Chattahoochee, Marion and Talbot Counties, GA.

Crystalline basement rocks in the study area are part of the Uchee terrane, a Neoproterozoic (620– 640 Ma) peri-Gondwanan sequence correlated with the Carolina superterrane by some workers (Steltenpohl et al., 2008). Amphibolite facies metamorphic rocks with Carboniferous (~300 Ma) zircon overgrowth indicates Alleghenian accretion to Laurentia (Steltenpohl et al., 2008) (Fig. 5). In the immediate vicinity of the unconformity, the Uchee terrane is comprised of the Phenix City Gneiss, Moffits Mill Schist, and Columbus Metamorphic Complex (Hanley and Steltenpohl, 1997; Steltenpohl et al., 2008). Basement rocks within the study area consist primarily of orthoamphibolite, orthogneiss, and paragneiss, as well as a limited amount of schist.

Immediately south of the CPU in the LCRV and stratigraphically above the basement is the Tuscaloosa Formation. The formation is named for exposures near Tuscaloosa, Alabama, where it has been defined as the Tuscaloosa Group. Monroe et al. (1946) identify four units within the Tuscaloosa in western Alabama, which from oldest to youngest consist of the Cottondale, Eoline, Coker, and Gordo Formations. Later work by Drennen (1953) reduced the number of formations within the western Tuscaloosa Group to two, keeping only the Coker and Gordo Formations. Averaging 250ft (76.2m) in thickness in the LCRV, the Tuscaloosa Formation reaches a maximum thickness of ~433ft (132m) at Ft. Benning, GA (Marsalis and Friddell, 1975). In western Georgia, the Tuscaloosa Formation can be divided into a basal paleosol unit and upper sand unit. The paleosol is a saprolitic remnant resulting from intense, tropical weathering of the underlying crystalline basement and is separated from overlying fluvial sands-conglomerates by an unconformity (Fig. 2). In the study area, the paleosol unit ranges from 1m to >10m in thickness and is commonly a reddish-orange, sandy or silty clay exhibiting yellow-white mottling.

Figure 5: Geologic map of Uchee and adjacent terranes (Steltenpohl et al., 2008).

Figure 5: Geologic map of Uchee and adjacent terranes (Steltenpohl et al, 2008).



Pedotubules and other pedological features of the paleosol led Sigleo and Reinhardt (1988) to argue it represents the B-horizon of a residual soil which formed on local crystalline rocks of the Uchee terrane in a Late Cretaceous subtropical or tropical environment. Above the paleosol, Cenomanian to Santonian (100.5 - 83.6 Ma, timescale used herein from Cohen et al., 2013) clastics of the Tuscaloosa Formation are units consisting of poorly-sorted, coarse grained, sub-angular sands and gravels in a kaolin matrix (Marsalis and Friddell, 1975) which were deposited in a fluvial system and are characterized by their high quartz content, kaolin matrix, and fining upward sequences. The coarse-grained, sub-angular, and poorly sorted character of the sediments indicates a proximal source. Fining upward sequences within the formation are the result of channel filling with decreasing slope as streams transitioned from highlands to coastal regions (Smith, 1984). Quartzite clasts and pebbles of rare gneiss in the Tuscaloosa Formation are consistent with derivation of sediment from local quartzofeldspathic gneiss of the Columbus Metamorphic Complex, the nearby Pine Mountain belt and potentially Inner Piedmont-eastern Blue Ridge terranes farther north (Fig. 6). These inclusions provide evidence for erosion and incision of the underlying basement and paleosol by the fluvial system responsible for deposition of the Tuscaloosa, which allows for placement of the CPU within the Tuscaloosa, between the paleosol and the overlying sandstones, rather than between the basement and Tuscaloosa Formation.



Figure 6: Clasts within the Tuscaloosa Formation. Left image—locally derived pisoliths. Right image—locally derived gneiss pebbles. Images courtesy of Dr. Bill Frazier.

Lying disconformably above the Tuscaloosa Formation is the Santonian to Campanian Eutaw Formation (86.3 – 72.1 Ma). The Eutaw is comprised of two sub-units, a basal coarse-grained, feldspathic quartzose sand and upper light gray to black micaceous, carbonaceous, fossiliferous silt, sand and clay layers (Marsalis and Friddell, 1975). The Eutaw Formation formed in a near shore, estuarine environment and represents the first sediments in the exposed LCRV to have formed in a fully marine setting (Fig. 7) (Frazier, 1996).

The characteristics of sediment within the Eutaw Formation do not represent solely autochthonous recycling of Tuscaloosa sediments, but indicate additional transport processes sourcing crystalline rocks predating the Cenomanian stage. Specifically, the variety of metamorphic minerals in the Eutaw Formation indicates the continued presence of nearby highlands during the Santonian age.

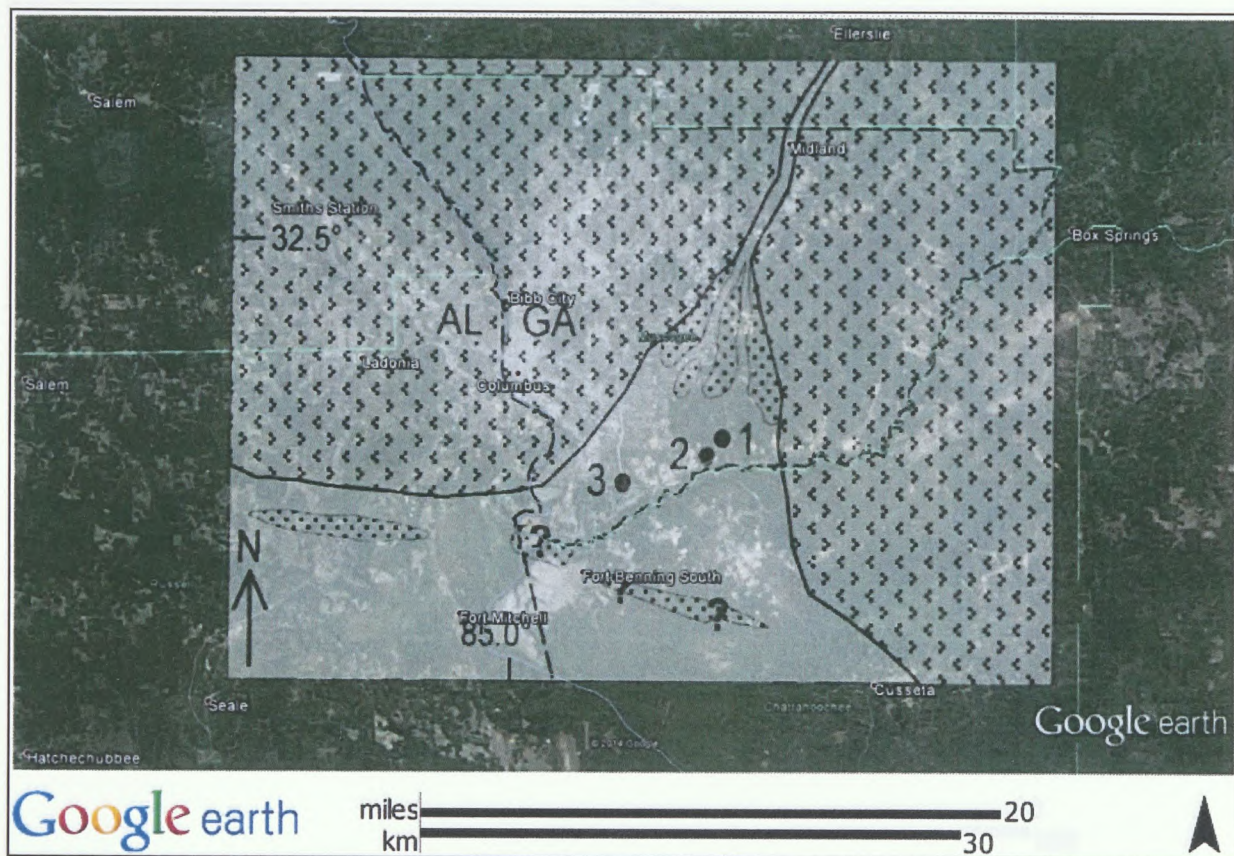


Figure 7: Paleoenvironment of the Eutaw Formation of eastern AL and western GA, east of the Eutaw paleodivide (adapted from Frazier, 1996).

Two disparate drainage basins located in a similar position to the modern Coosa and Chattahoochee drainage basins (Fig. 8) are indicated by heavy mineral analysis (Fig. 9) of Eutaw Formation sediments (Osborne, 2013). The presence of a Santonian-Campanian paleodivide is consistent with a transition from sediments lacking high-grade metamorphic facies minerals east of the divide, within the modern LCRV, to sediments containing those minerals west of the divide. Coupled with paleotopographic analysis of the CPU, this indicates the possibility of a paleodrainage system spanning the interval of both Tuscaloosa and Eutaw Formation sedimentation (>25 m.y.).

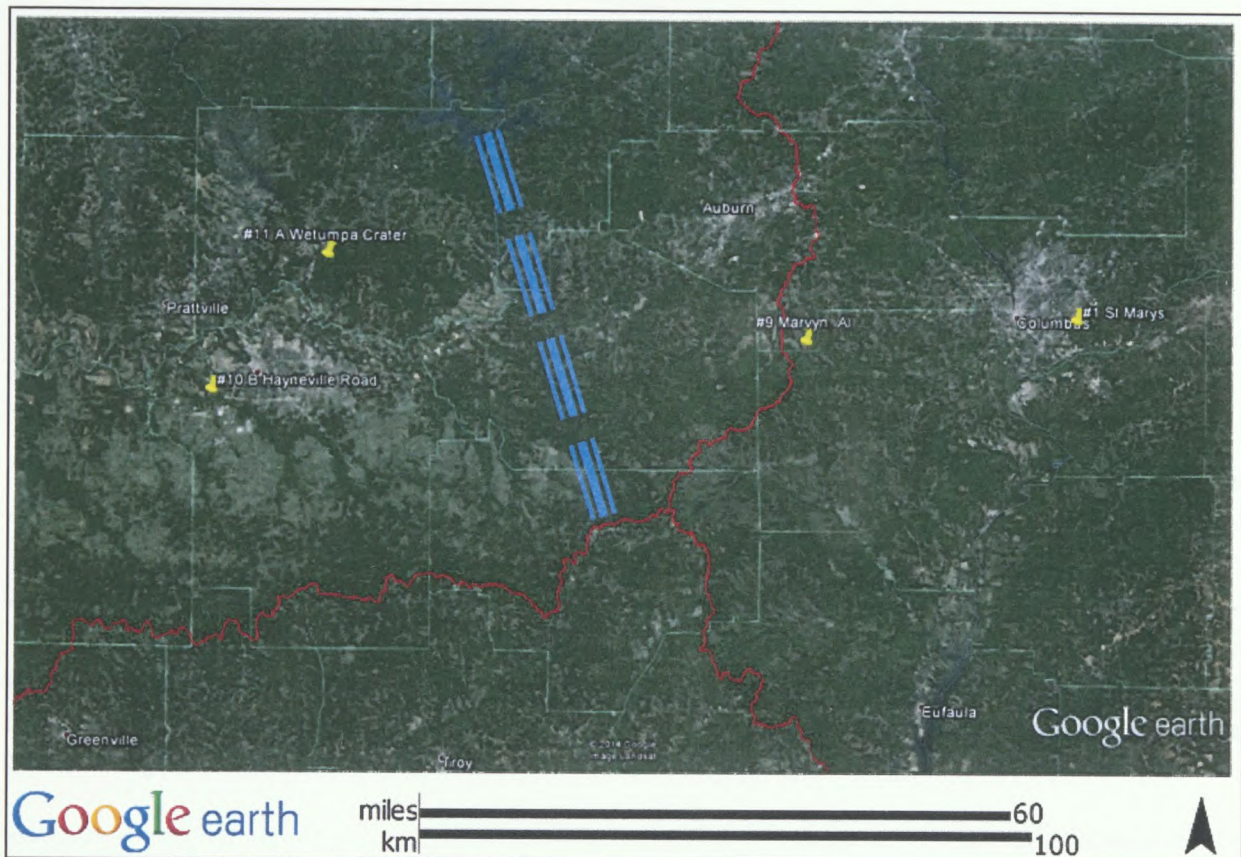


Figure 8: Selected stations from the Eutaw Formation between Montgomery, AL and Columbus, GA used for mineralogical provenance study (Osborne, 2013). Red lines show modern drainage boundaries. Blue line shows approximate location of an Upper Cretaceous paleodivide in the Eutaw drainage system.

Geological study of the Eutaw within the LWD project can be approached by focusing the center of underlying Piedmont basement, where weathered paleosols developed on that basement with overlying Coastal Plain sediments. In locations where the contact surface has obscured directly, sampling of the bedrock is possible by examining the location of Cretaceous sediments and basement rocks to geologically correlate them and interpreting the contact between sediments and rocks above and below the weathering. Using the known of directly observed and interpreted points on the weathering, a model reconstruction of the Upper Cretaceous paleodivide can be generated using GID software.

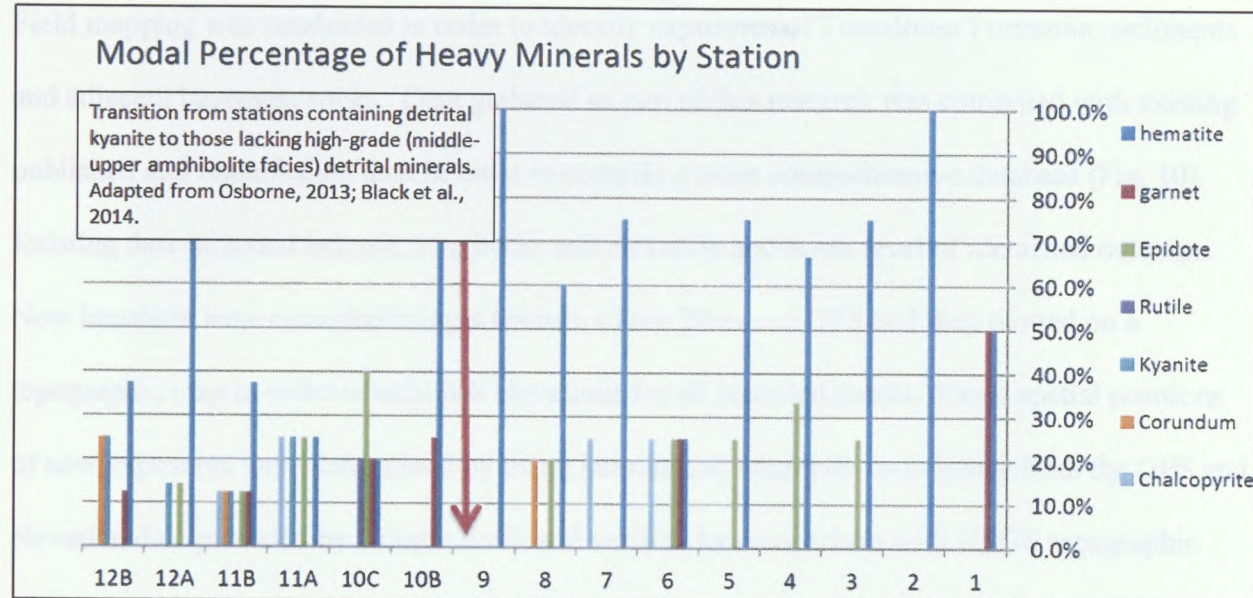


Figure 9: Heavy mineral modes in selected Eutaw Formation localities identifying a potential Upper Cretaceous paleodivide west of the AL-GA state line (adapted from Osborne, 2013; Black et al., 2014).

Methods

Paleotopography of the CPU within the LCRV region can be approximated by locating the contact of underlying Piedmont basement, and/or residual paleosols developed on that basement, with overlying Coastal Plain sediments. In locations where the contact cannot be observed directly, mapping of the contact is possible by constraining the location of Tuscaloosa sediments and basement rocks in proximity to one another and interpolating the contact between adjacent points above and below the unconformity. Using the location of directly observed and interpolated points on the unconformity, a visual representation of the Upper Cretaceous paleosurface can be constructed using GIS software.

Field mapping was conducted in order to identify exposures of Tuscaloosa Formation sediments and adjacent basement rocks. Data gathered as part of this research was combined with existing published and unpublished data in order to compile a more comprehensive database (Fig. 10). Existing data included latitude, longitude, and elevation above sea level of identified outcrops. New locations were recorded using a Garmin eTrex 20 model GPS and then plotted on a topographic map in order to establish elevations for all recorded points. Exact spatial positions of new exposures were determined by using latitude and longitude coordinates from the GPS and elevation data provided by Google Earth and verified by comparison with USGS topographic maps. Stated vertical and horizontal accuracy of the Garmin eTrex GPS is approximately 40ft (12.2m). Elevation data provided by the GPS was discarded due to the degree of inaccuracy and lack of correspondence with available topographic map data and Google Earth. Model and accuracy of the GPS unit used in previous data collection is unknown. USGS topographic map accuracy standards require an accuracy of 40 ft (12.2m) in the horizontal axes and 5 ft (1.5m) in the vertical axis (USGS, 1999). Google Earth has a previously tested accuracy of approximately 5.9 ft (1.8m) in the horizontal axes and 5.7 ft (1.73m) in the vertical axis (Mohammed et al., 2013).

In places where the contact between rocks of the Piedmont, or the paleosol developed on those rocks, and sedimentary units of the Tuscaloosa Formation could not be observed directly, the location of the contact was interpolated by selecting the mean elevation between the nearest identified Piedmont and Tuscaloosa Formation exposures (Fig. 11). The resulting interpolated points for the unconformity were then plotted along with observed points (Figs. 12 and 13) on the contact and contoured in order to create a paleotopographic surface of the Upper Cretaceous CPU in the vicinity of the LCRV (Fig. 14).

Figure 10: GPS data and plotting data points.

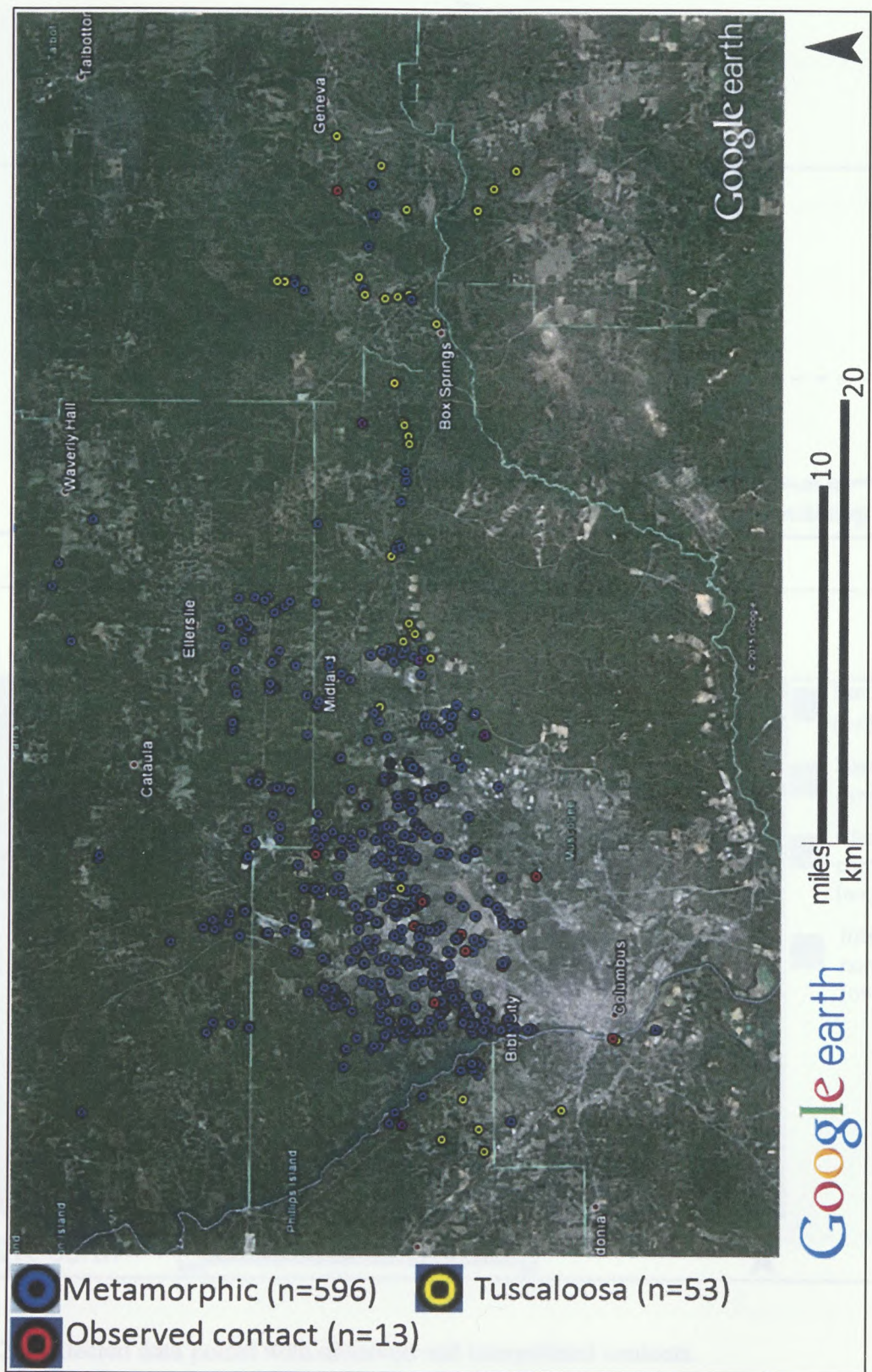


Figure 10: All new and existing data points.

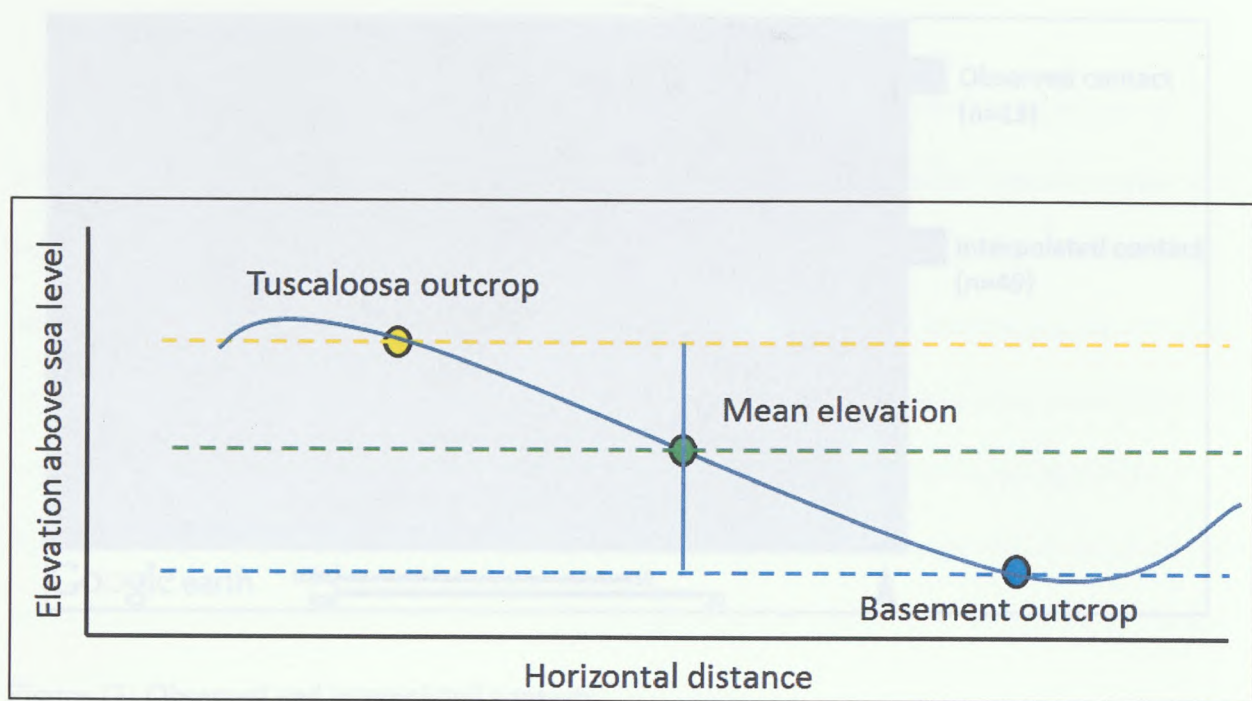


Figure 11: Method for interpolating contact elevations.

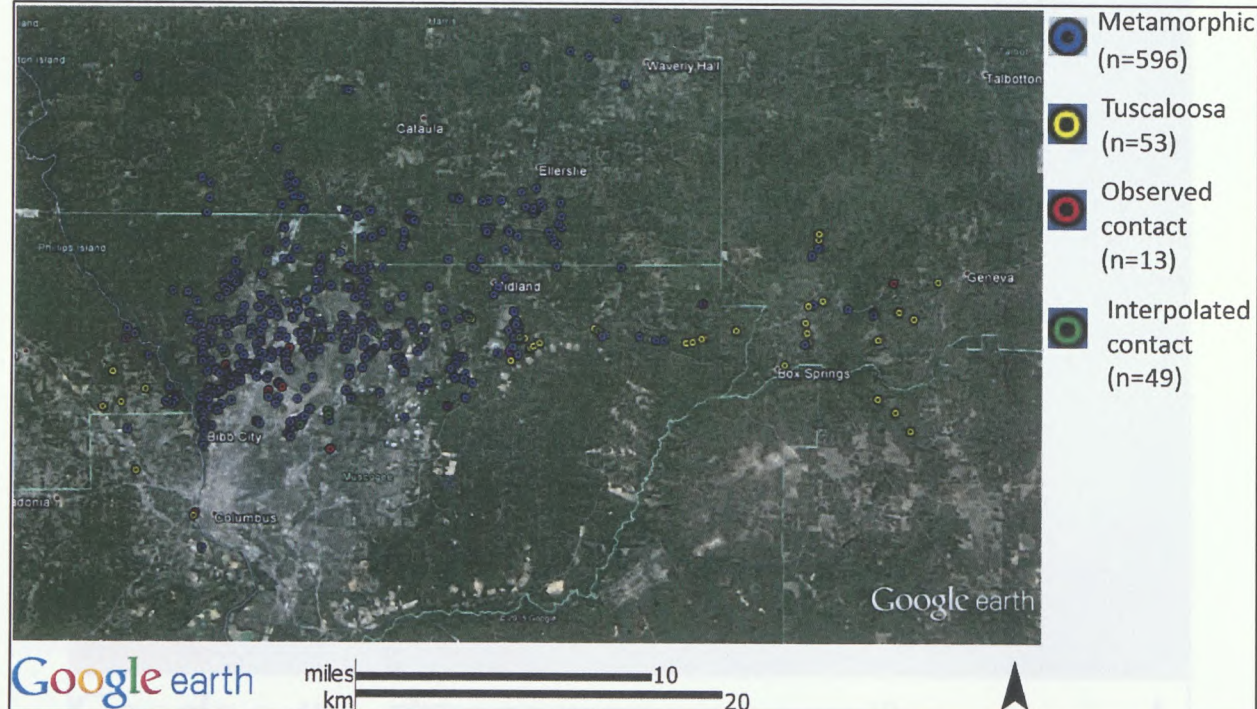


Figure 12: Collected data points with observed and interpolated contacts.

FIGURE 12: Summary of the contacts on the study. Blue circles show the location of potential polymetamorphic.

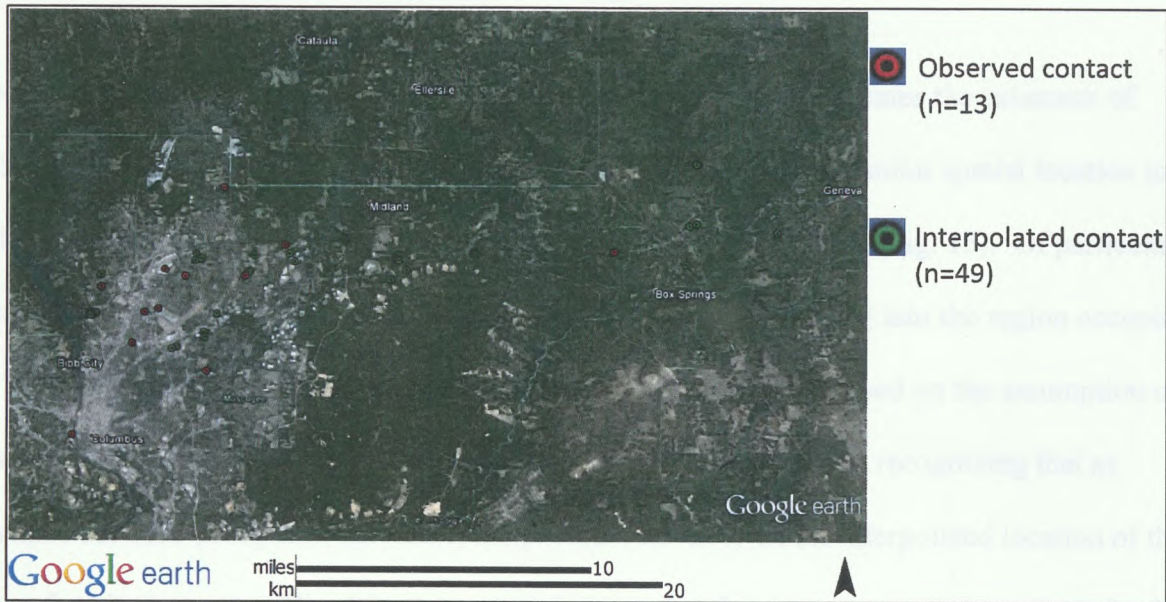


Figure 13: Observed and interpolated contacts.

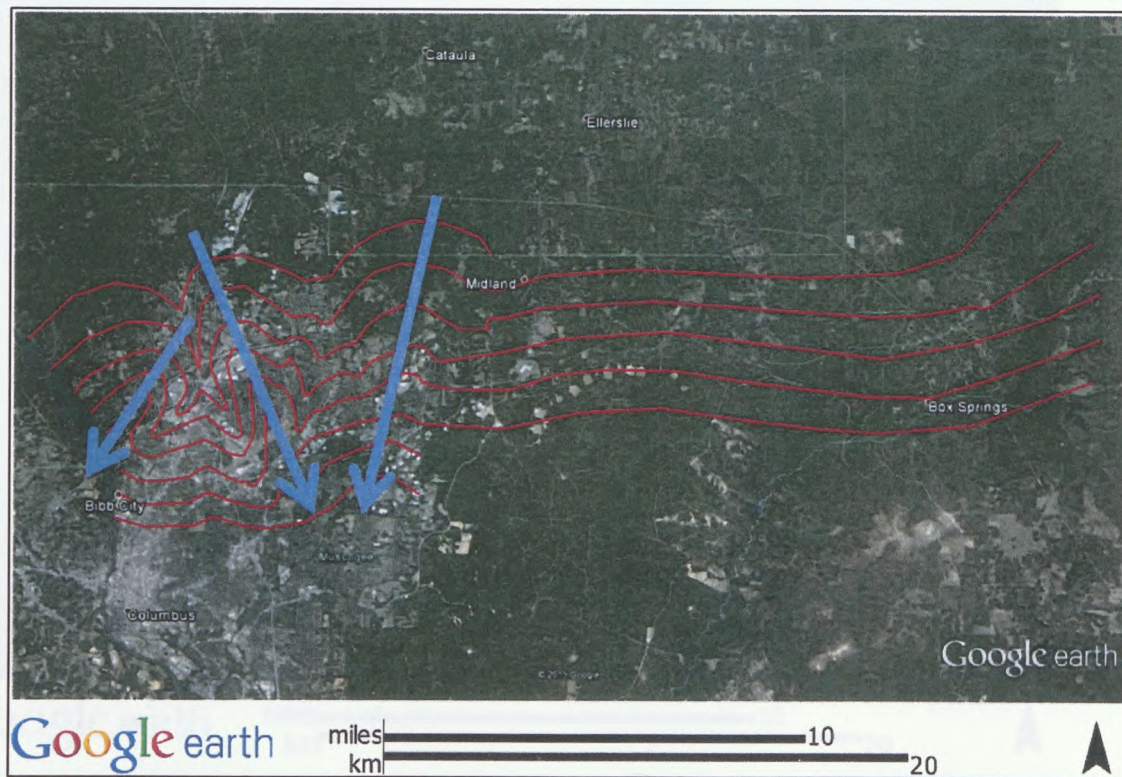


Figure 14: Contours (15m interval) on the CPU. Blue arrows show the location of potential paleochannels.

Contouring observed and interpolated points on the unconformity indicates the existence of paleochannels in the sub-Tuscaloosa Formation surface occupying a similar spatial location to a paleodrainage system identified within the overlying Eutaw Formation (Fig. 15). Of particular interest are the eastern and central channels which appear to be feeding into the region occupied by the future Eutaw Formation estuary. Interpolation of contacts is based on the assumption of a reasonably planar surface along the unconformity over short distances, recognizing that as distance between data points increases, the potential for error on the interpolated location of the unconformity increases (Fig. 16). As such, it is important that one or more independent checks be established on the interpolation method presented here.

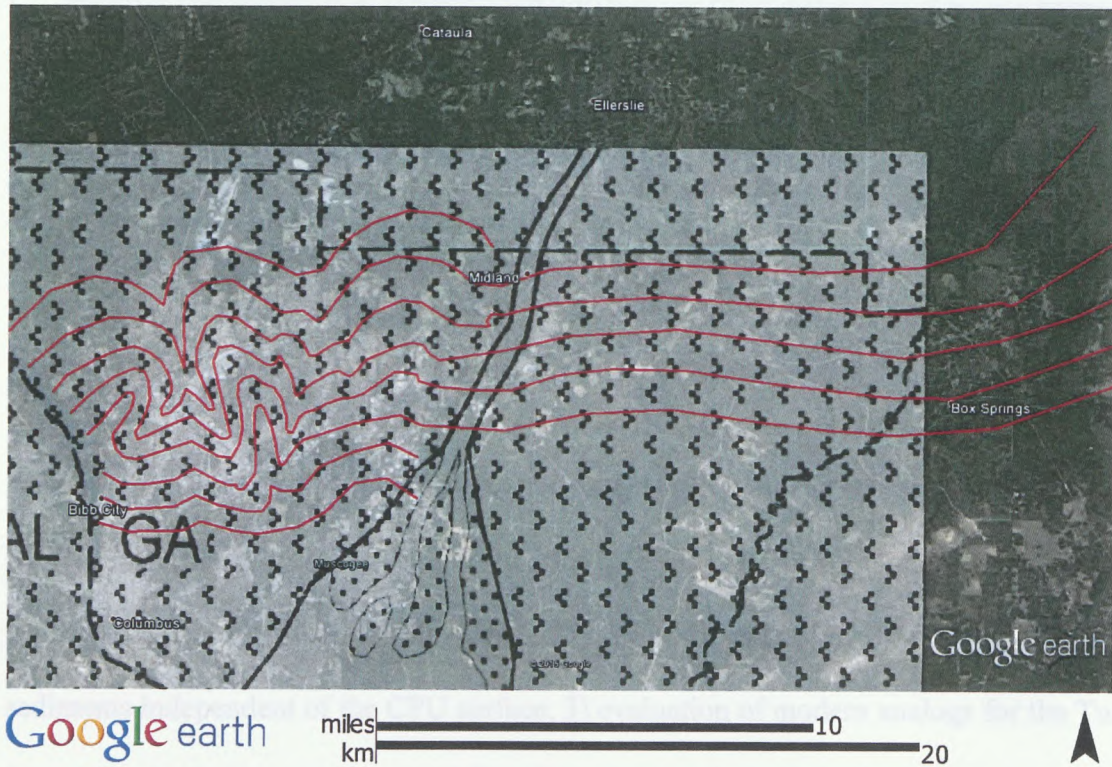


Figure 15: Comparison of Eutaw paleochannel with proposed Tuscaloosa paleochannel (adapted from Frazier, 1996).

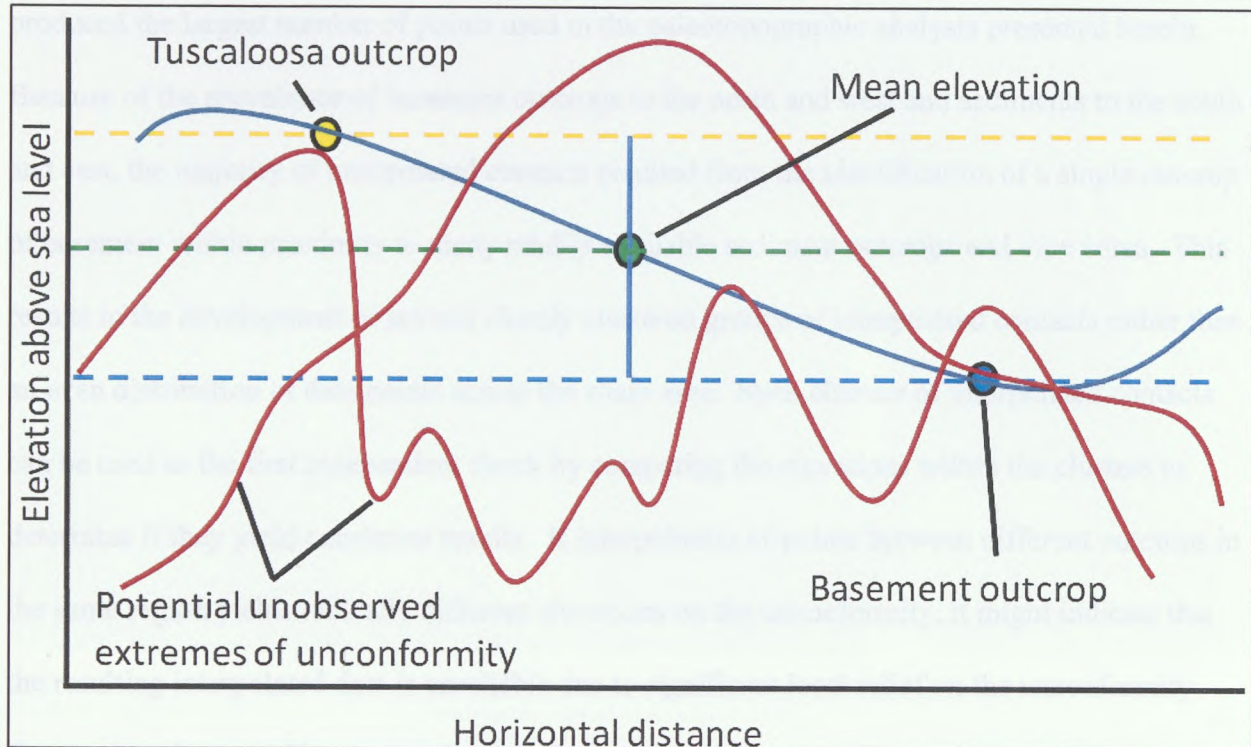


Figure 16: Potential pitfall of interpolating contact elevations. Red lines depict extremes in the geometry of the unconformity between observed points below (blue circle) and above (yellow circle) the unconformity. The actual unconformity could lie above or below the interpolated (green circle) position of the unconformity.

Independent Checks

A series of independent checks designed to validate the results of this study have been implemented. They consist of 1) examination of clusters of interpolated contacts to determine the consistency of interpolated elevations, 2) contouring of basement rocks and Tuscaloosa sediments independent of the CPU surface, 3) evaluation of modern analogs for the Tuscaloosa's depositional paleoenvironment, and 4) sedimentary analysis of the local Tuscaloosa Formation.

Due to the difficulty in locating observable contacts on the CPU, interpolation of contacts produced the largest number of points used in the paleotopographic analysis presented herein. Because of the prevalence of basement outcrops to the north and west and sediments to the south and east, the majority of interpolated contacts resulted from the identification of a single outcrop of basement within proximity to many readily available sediment outcrops and vice versa. This results in the development of several closely clustered groups of interpolated contacts rather than an even distribution of data points across the study area. Such clusters of interpolated contacts can be used as the first independent check by comparing the elevations within the clusters to determine if they yield consistent results. If interpolation of points between different outcrops in the same region yields radically different elevations on the unconformity, it might indicate that the resulting interpolated data is unreliable due to significant local relief on the unconformity. Contouring clusters of interpolated points, however, yield reasonably consistent changes in elevation across the study area and indicate reliability of interpolated data (Fig. 17).

Contouring basement rocks and Tuscaloosa sediments independently from the CPU also indicates a degree of consistency for contours on the CPU. Most sample locations do not lie directly on the contact, with the actual unconformity at an unknown distance above or below the observed station. If observed exposures used in interpolation lie in close proximity to the actual unconformity, then independently contouring elevations of exposed basement and Tuscaloosa Formation sediment should yield similar contour patterns to that of the interpolated CPU surface.

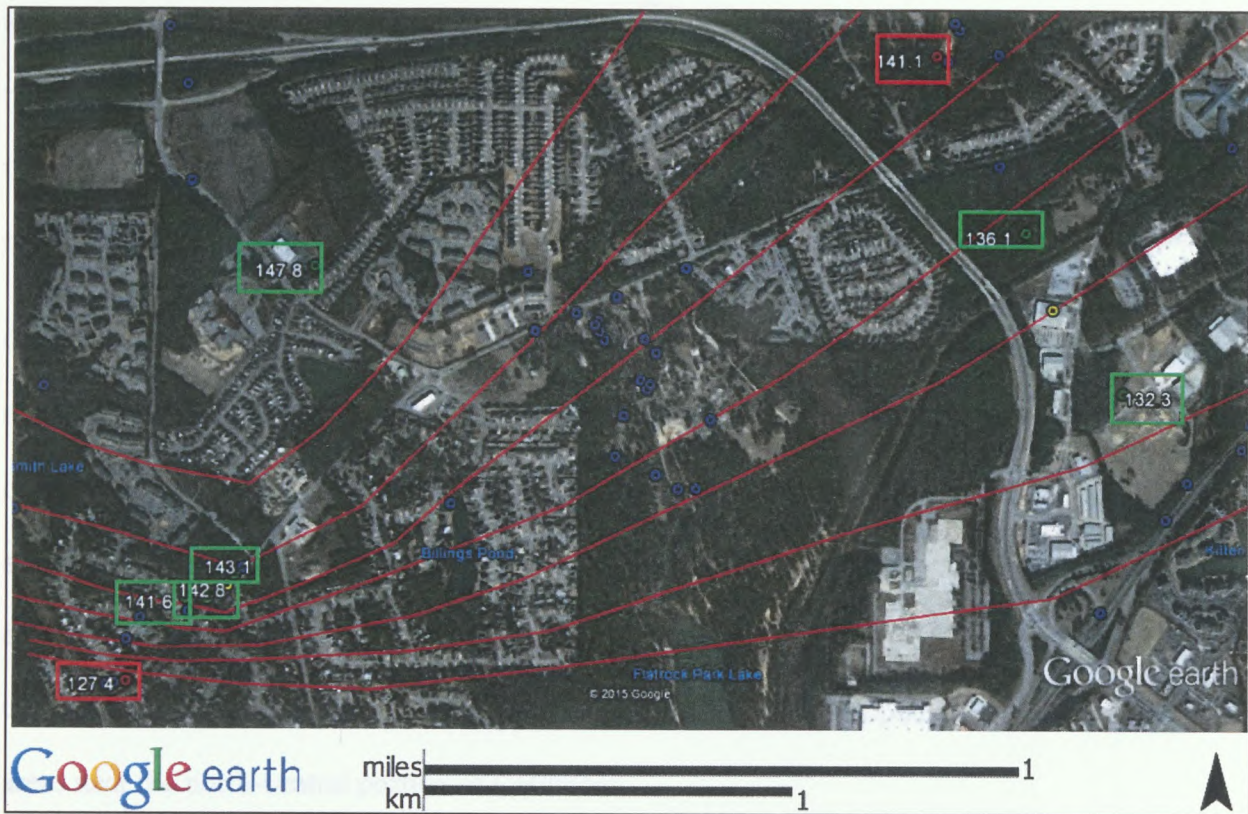


Figure 17: Cluster of interpolated points showing expected elevation consistency. Red lines indicate 3m contour interval. Green boxes are interpolated contacts. Red boxes are observed contacts. Numbers indicate elevations in meters above sea level for each identified point.

Sampling of data points that include basement or Tuscaloosa Formation clastics produces results that are somewhat random in terms of elevation, due to the nature in which sampling occurs. Recorded elevations are a result of outcrop availability and are controlled by factors which include both weathering in a subtropical environment and extensive urban development. However, the character of exposure is also affected by the position of the CPU relative to modern topography. If outcrops were truly random, then contouring of basement elevation points should produce a different surface than contouring of elevation points on Tuscaloosa Formation clastics. However, contouring of data points on the basement independent of those data points on sedimentary units of the Tuscaloosa Formation does not produce two random

surfaces, but rather surfaces with similar paleotopography, specifically the indication of paleovalleys in the western portion of the study area. Relief on the unconformity itself is, therefore, more likely to be the result of actual paleotopography rather than relics produced by outcrop.

Contouring of basement produces significant detail north and west of the unconformity, where outcrops of basement are most prevalent. Although basement outcrop abundance decreases east of the city of Columbus, limited basement data mirrors that of the overlying Tuscaloosa sedimentary sequences and does not indicate the existence of significant paleochannels in the eastern region of the study area (Fig. 18). Evidence for a potential paleochannel occurs within the Midland area at the eastern boundary of Columbus' urban development, as well as in several areas near the north-central portion of Columbus.

Contouring of Tuscaloosa Formation sediments produces similar results, with paleotopography indicating channels in the western, but not eastern region of the study area. Similar contour patterns from both basement and sediment exposures in the central and western portions of the LCRV indicate prominent paleovalleys in the western region of the study area are not the result of random sampling, but are instead a function of actual relief on the Upper Cretaceous surface (Fig. 19).

Figure 18: Contours (10m interval) of elevation data for crosscutting basement rocks (grayscale).

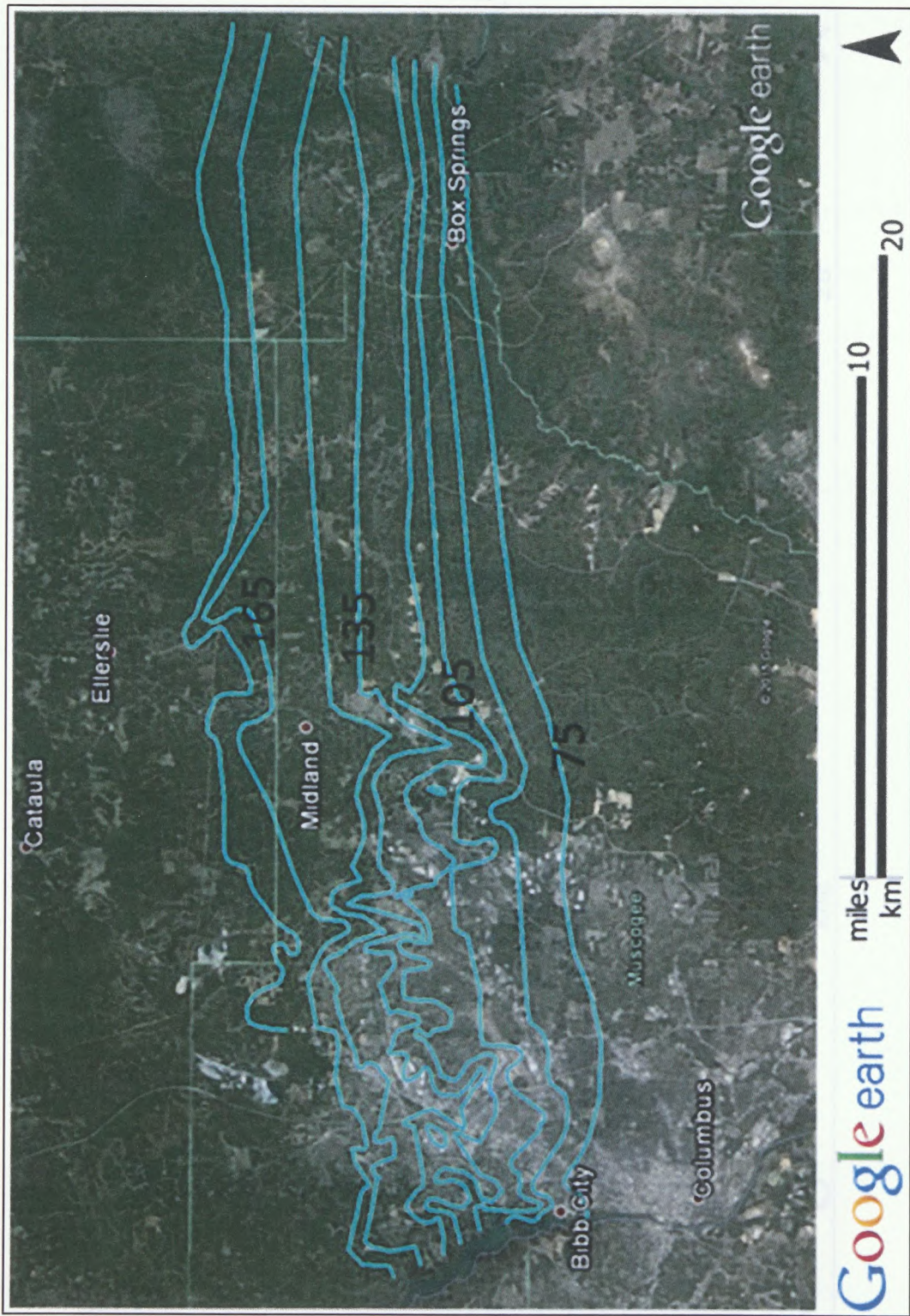


Figure 18: Contours (15m interval) of elevation data for metamorphic basement rocks-paleosol.

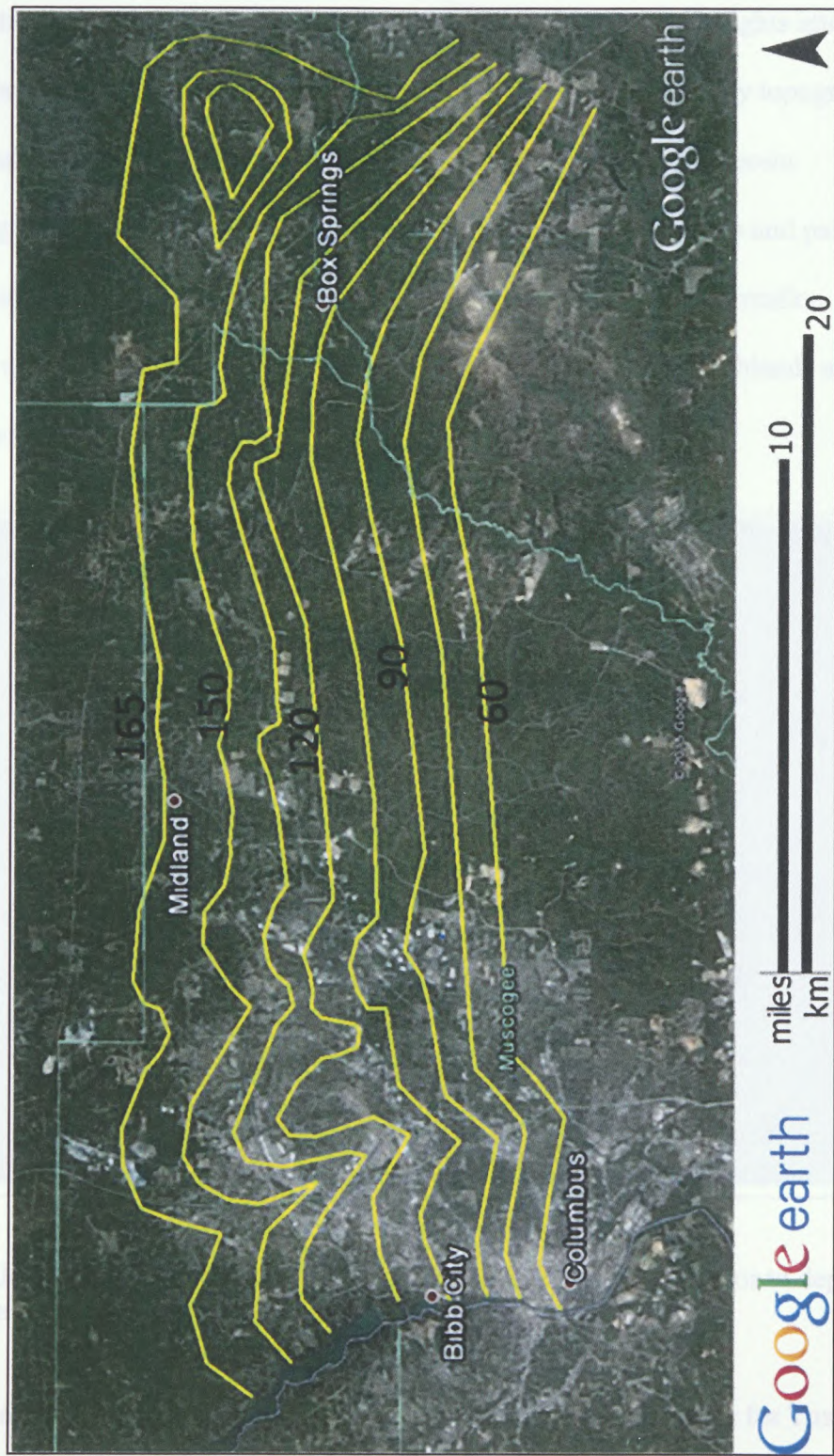


Figure 19: Contours (15m interval) of elevation data for Tuscaloosa Formation clastics.

Topographic

Figure 19: Contours (15m interval) of elevation data for Tuscaloosa Formation clastics.

The examination of modern analogous environments may also provide insights into conditions of the likely depositional environment of the Tuscaloosa Formation, especially topographic relief, and provide an independent check on the interpolation method presented herein.

Sedimentological analysis of Tuscaloosa Formation sedimentary sequences and paleotectonic reconstructions of North America indicate sediments of the Tuscaloosa Formation were deposited by a braided fluvial system in proximity to both the sourcing highlands and coast at tropical latitude (Fig. 20).



Figure 20: Paleogeographic reconstruction North America immediately prior to deposition of the Tuscaloosa Formation, ca. 105 Ma (Blakey, 2013).

Topographic relief in modern analogues to the inferred depositional setting for Tuscaloosa Formation sediments immediately above the CPU allows for comparison of relief in the two settings. Three rivers in environmental settings analogous to the depositional environment for

the Tuscaloosa Formation were selected near the southeastern coast of Brazil in the state of Santa Catarina (Fig. 21). Similarities between this modern setting and inferred characteristics of the depositional environment for the Tuscaloosa Formation in the vicinity of the LCRV include a tropical/subtropical environment between 0° and 30° latitude, and the presence of braided stream systems proximal to both source highlands and the coastline. Calculation of the longitudinal slopes of the rivers and the paleochannels yields similar results. Average longitudinal slopes of the rivers are approximately 248 m/km, while slopes of the identified paleochannels are approximately 312 m/km. Comparison of the longitudinal slopes of the modern river valleys and the eastern-most paleochannel over equidistant lengths (2.6 km) can be seen in Figure 22. Cross-valley width of the eastern-most paleochannel is approximately 2.6 km. Comparison of the cross-valley elevation profiles of the modern river valleys over the same distance yields similar results (Fig. 23).

Figure 21: Analog for Tuscaloosa Formation depositional environment, southeastern Brazil.



Figure 22: Comparison of elevation changes for the three Brazilian rivers and the eastern-most LCRV paleochannel over a constant distance.



Figure 21: Analog for Tuscaloosa Formation depositional environment, southeastern Brazil.

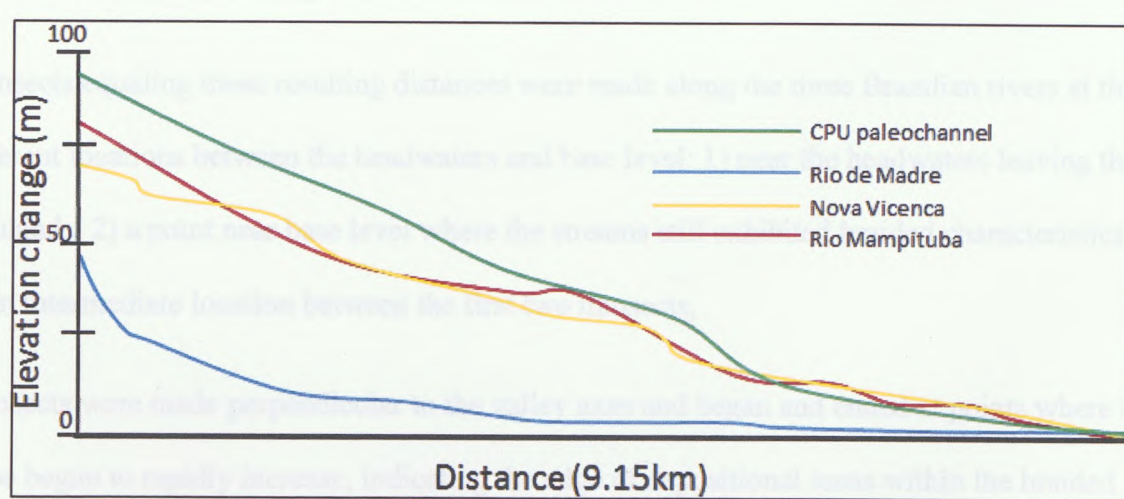


Figure 22: Comparison of elevation changes for the three Brazilian rivers and the eastern-most CPU paleochannel over a constant distance.

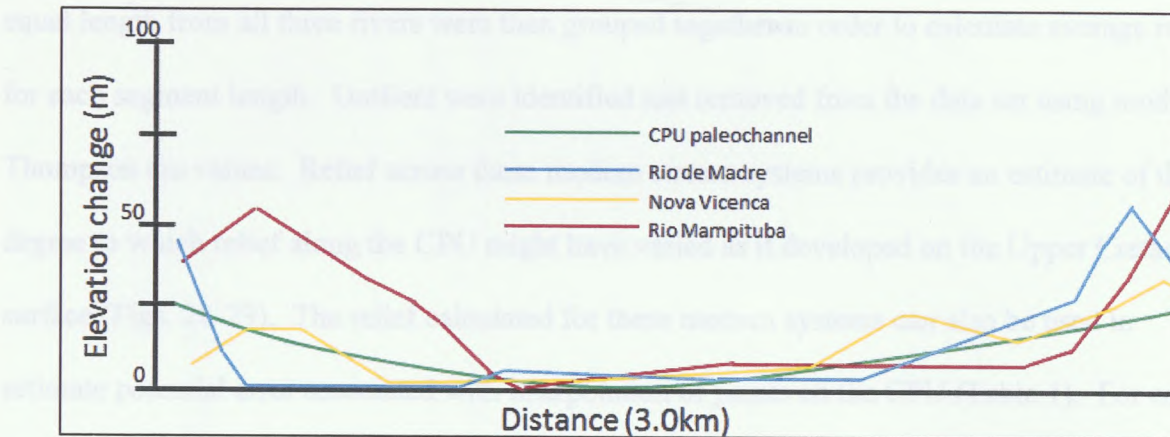


Figure 23: Comparison of the cross-valley profiles of the three Brazilian rivers over a constant distance equal to the width of the eastern-most paleochannel.

Three rivers—Rio Mampituba, Rio de Madre, and an unnamed river near Nova Vicenca—were selected for comparison. Data gathered for this project was organized into three groups based on the distance between points used for interpolation (Table 1). Distances between stations used for interpolation were plotted according to separation distance between adjacent stations and grouped into four modes defined by the distance between stations used in interpolation: 122m, 305m, 442m, and 579m (Fig. 24).

Transects equaling these resulting distances were made along the three Brazilian rivers at three different locations between the headwaters and base level: 1) near the headwaters leaving the highlands, 2) a point near base level where the streams still exhibited braided characteristics, and 3) an intermediate location between the first two transects.

Transects were made perpendicular to the valley axes and began and ended at points where the slope began to rapidly increase, indicating the edge of depositional areas within the braided stream systems (Fig. 25). The maximum and minimum elevations of each transect length (122m, 305m, 442m, and 579m) were used to determine the total relief of each segment. Transects of

equal length from all three rivers were then grouped together in order to calculate average relief for each segment length. Outliers were identified and removed from the data set using modified Thompson tau values. Relief across these modern stream systems provides an estimate of the degree to which relief along the CPU might have varied as it developed on the Upper Cretaceous surface (Figs. 26-29). The relief calculated for these modern systems can also be used to estimate potential error associated with interpolation of points on the CPU (Table 1). For each of the transect lengths, the average relief provides an approximation of the plus/minus error value on placement of the interpolated unconformity in terms of its elevation.



Figure 26: Plot of distances between physical locations used in interpolation. Groups of data points can be used for relief comparison in modern systems.

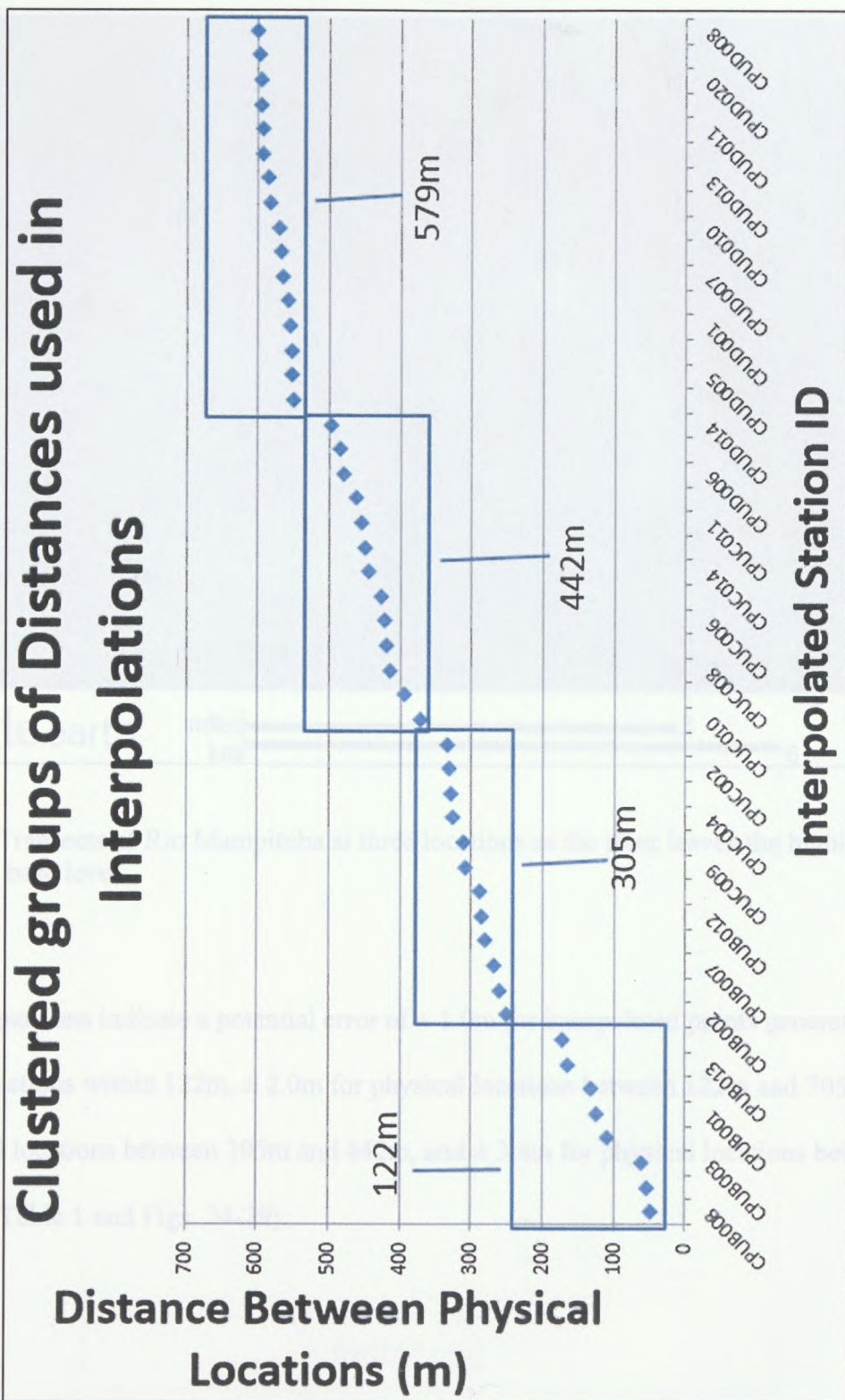


Figure 24: Plot of distances between physical locations used in interpolations. Groups of data points can be used for relief comparison to modern analogues.

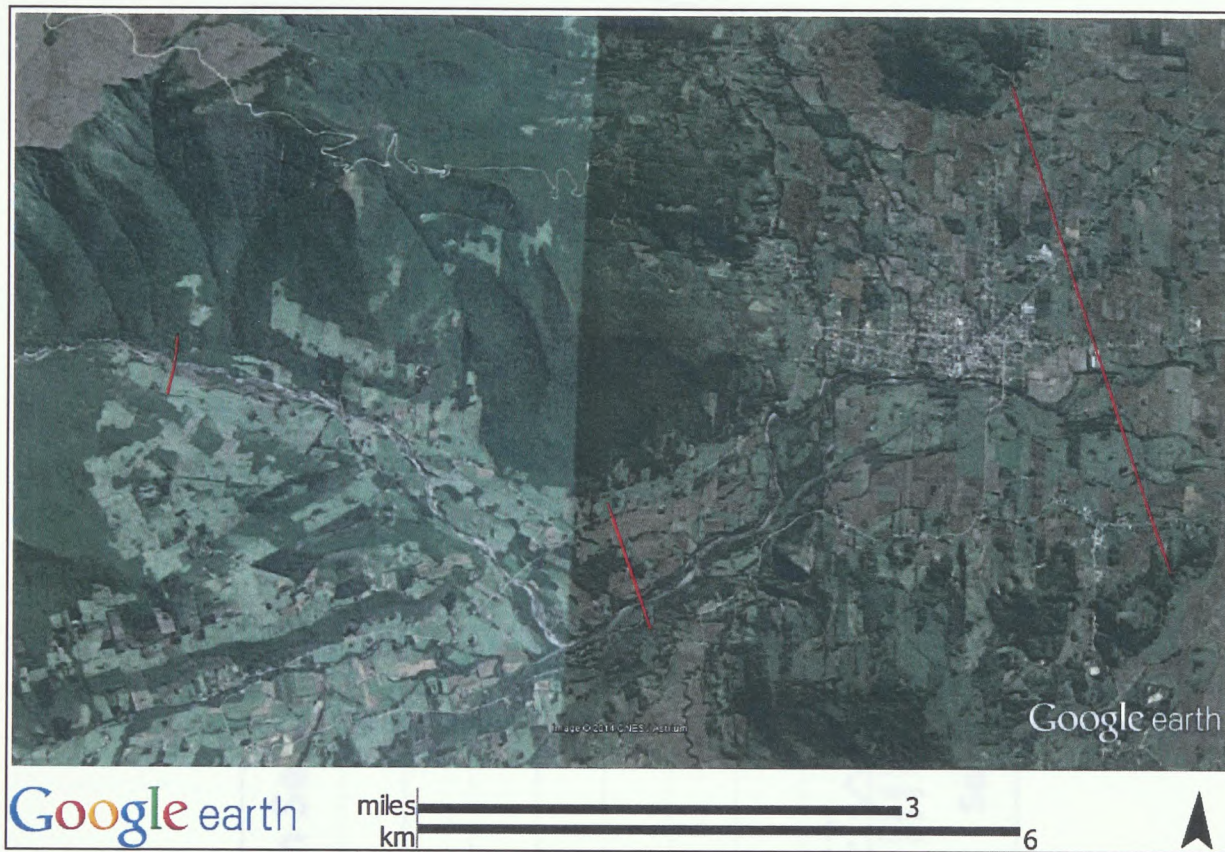


Figure 25: Transects of Rio Mampituba at three locations as the river leaves the highlands and approaches base level.

Relief comparisons indicate a potential error of $\pm 1.0\text{m}$ for interpolated points generated by physical locations within 122m, $\pm 2.0\text{m}$ for physical locations between 122m and 305m, $\pm 3.0\text{m}$ for physical locations between 305m and 442m, and $\pm 3.4\text{m}$ for physical locations between 442m and 579m (Table 1 and Figs. 24-29).

Figure 26: Plot of 122m transect segments versus total relief for each segment within Braulio River valleys used as modern analogues for paleochannels responsible for Tucanoite transportation and deposition. Average relief is $\pm 1.0\text{m}$ with outliers removed.

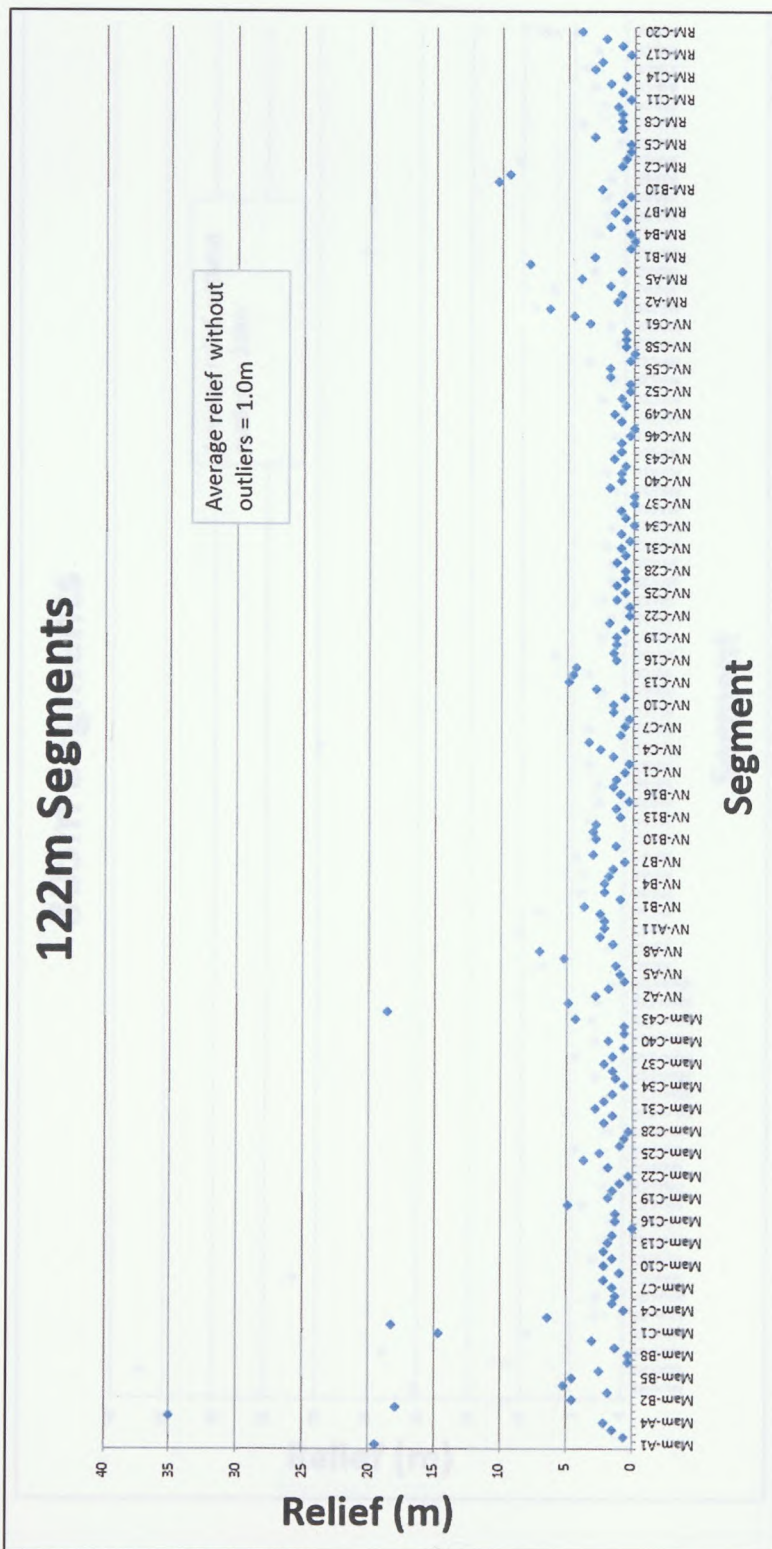


Figure 26: Plot of 122m transect segments versus total relief for each segment within Brazilian river valleys used as modern analogues for paleochannels responsible for Tuscaloosa transportation and deposition. Average relief is $\pm 1.0\text{m}$ with outliers removed.

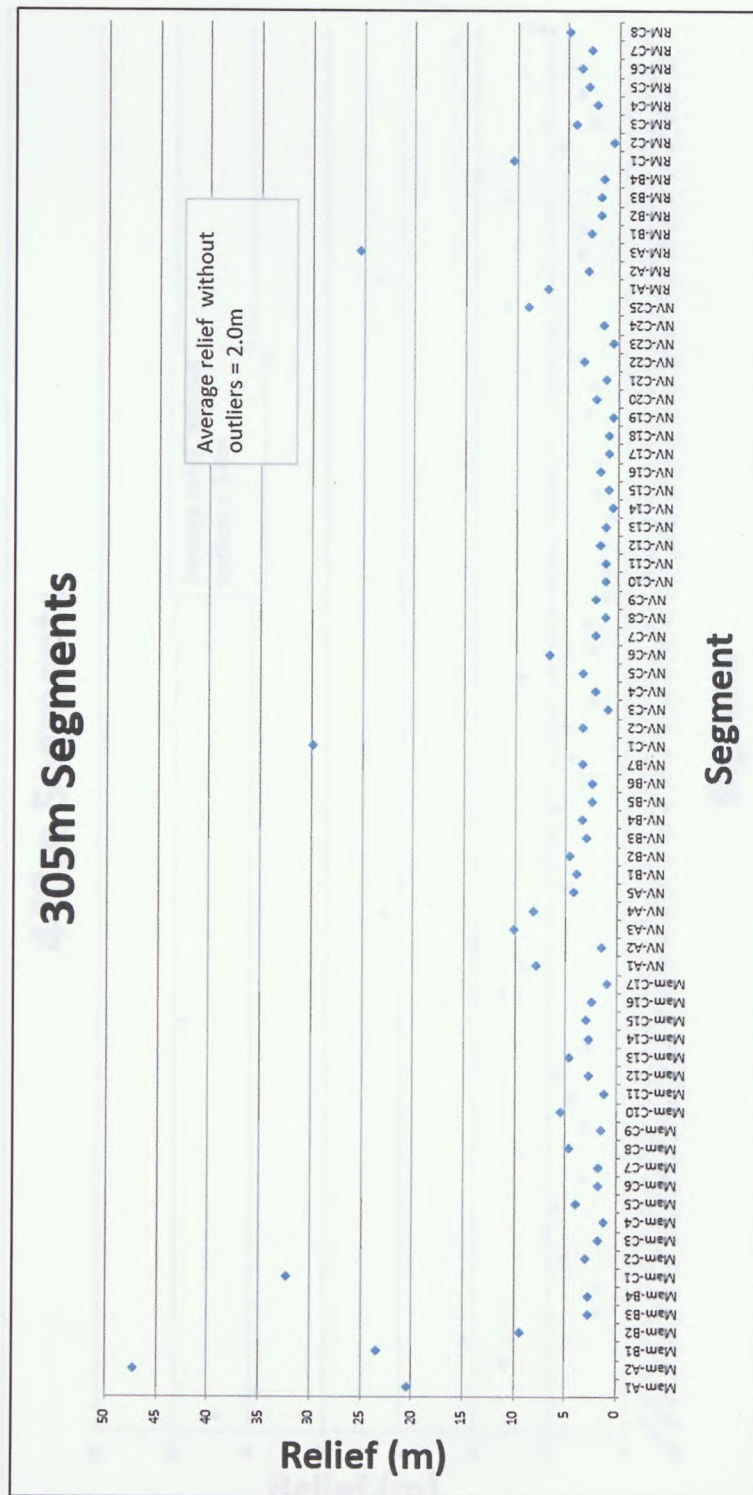


Figure 27: Plot of 305m transect segments versus total relief for each segment within Brazilian river valleys used as modern analogues for paleochannels responsible for Tuscaloosa transportation and deposition. Average relief is $\pm 2.0\text{m}$ with outliers removed.

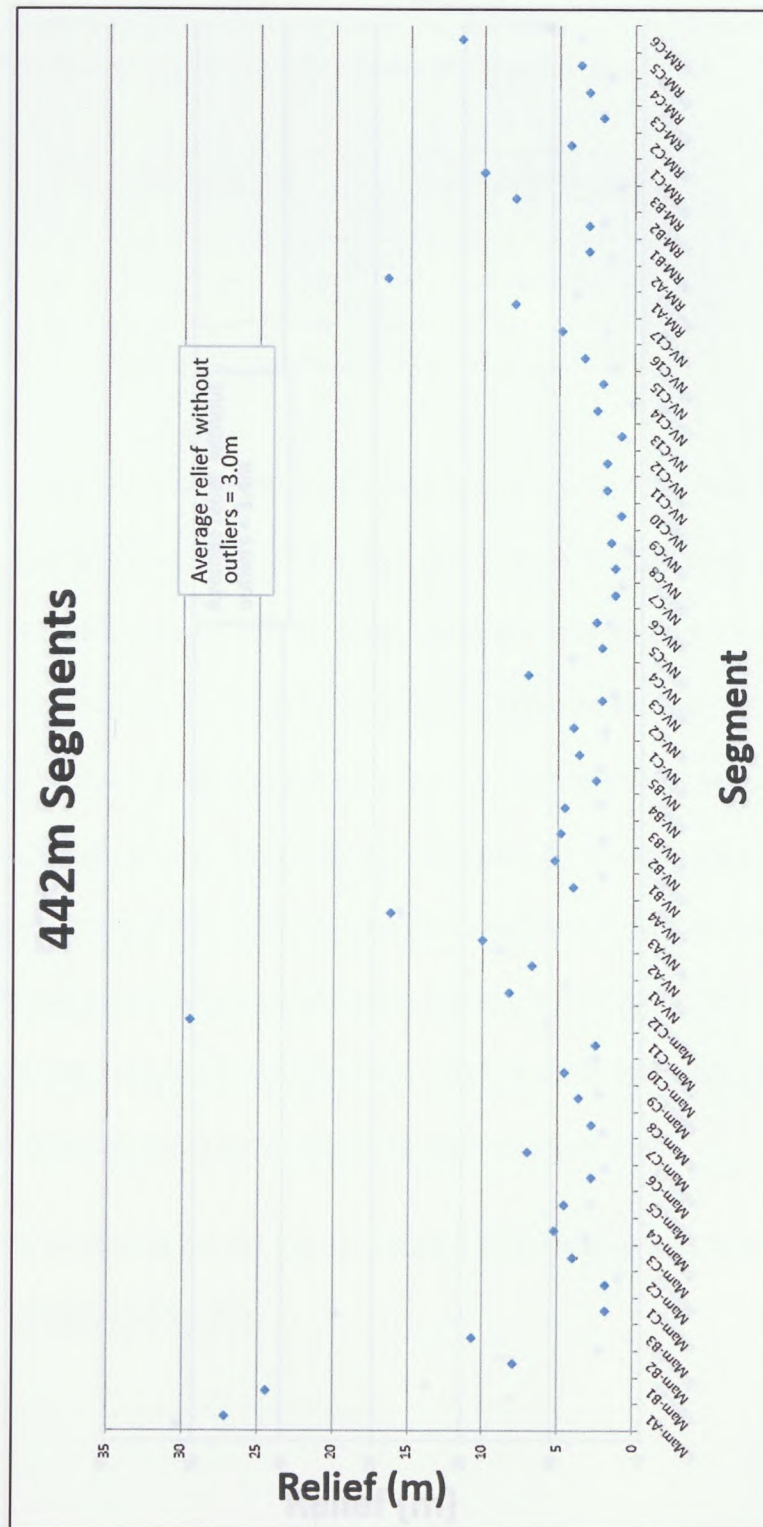


Figure 28: Plot of 442m transect segments versus total relief for each segment within Brazilian river valleys used as modern analogues for paleochannels responsible for Tuscaloosa transportation and deposition. Average relief is $\pm 3.0\text{m}$ with outliers removed.

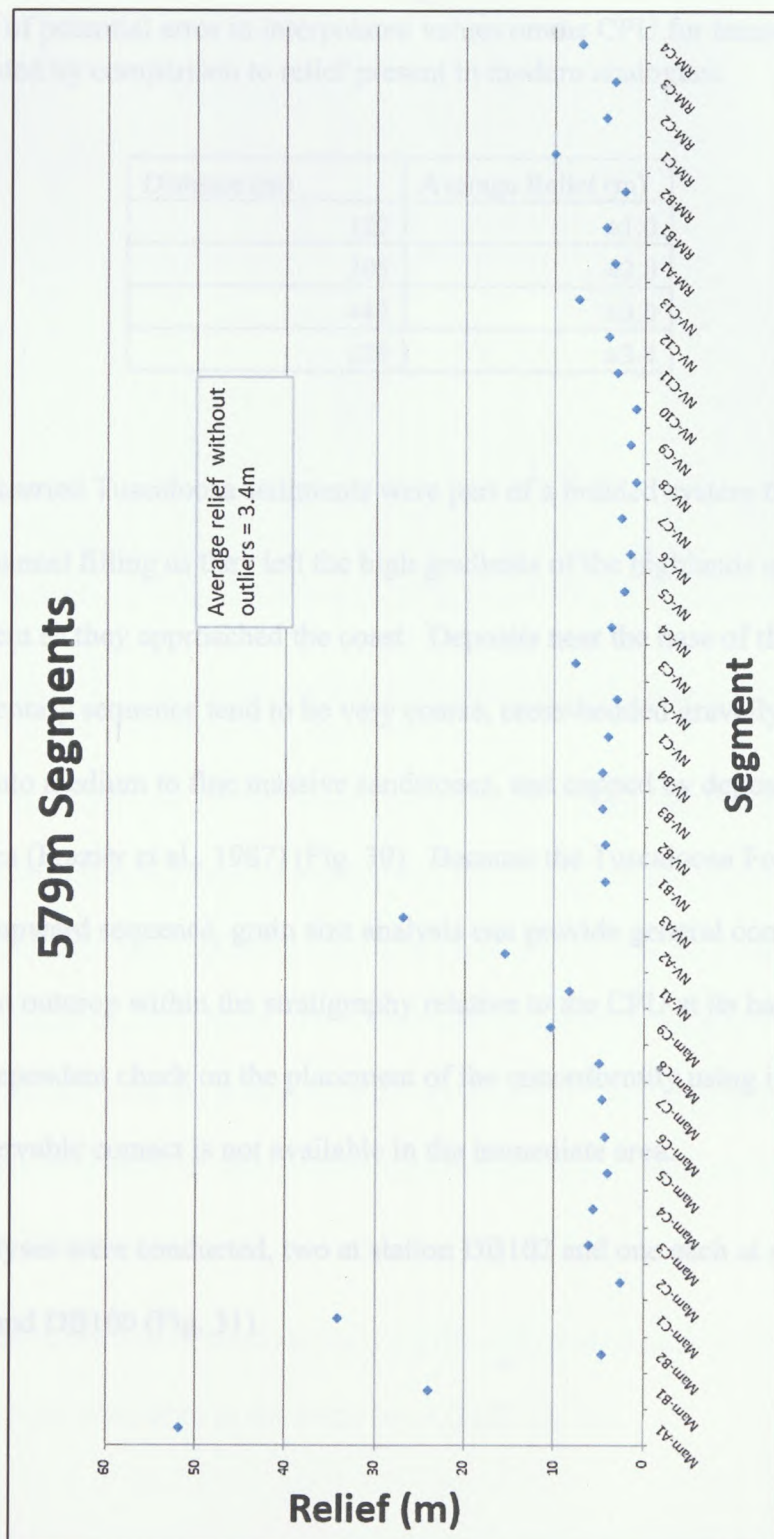


Figure 29: Plot of 579m transect segments versus total relief for each segment within Brazilian river valleys used as modern analogues for paleochannels responsible for Tuscaloosa transportation and deposition. Average relief is $\pm 3.4\text{m}$ with outliers removed.

Table 1: Amount of potential error in interpolated values on the CPU for transects of different lengths as calculated by comparison to relief present in modern analogues.

Distance (m)	Average Relief (m)
122	± 1.0
305	± 2.0
442	± 3.0
579	± 3.4

The streams that carried Tuscaloosa sediments were part of a braided system that resulted in deposition and channel filling as they left the high gradients of the highlands and began to decrease in gradient as they approached the coast. Deposits near the base of the Tuscaloosa Formation sedimentary sequence tend to be very coarse, cross-bedded gravelly sandstones, grading upward into medium to fine massive sandstones, and capped by deposits of massive, mottled mudstones (Frazier et al., 1987) (Fig. 30). Because the Tuscaloosa Formation represents an overall fining upward sequence, grain size analysis can provide general constraints on the location of a given outcrop within the stratigraphy relative to the CPU at its base. This provides a general and independent check on the placement of the unconformity using interpolation in the event that an observable contact is not available in the immediate area.

A total of six analyses were conducted, two at station DB102 and one each at stations DB039, DB043, DB088, and DB100 (Fig. 31).

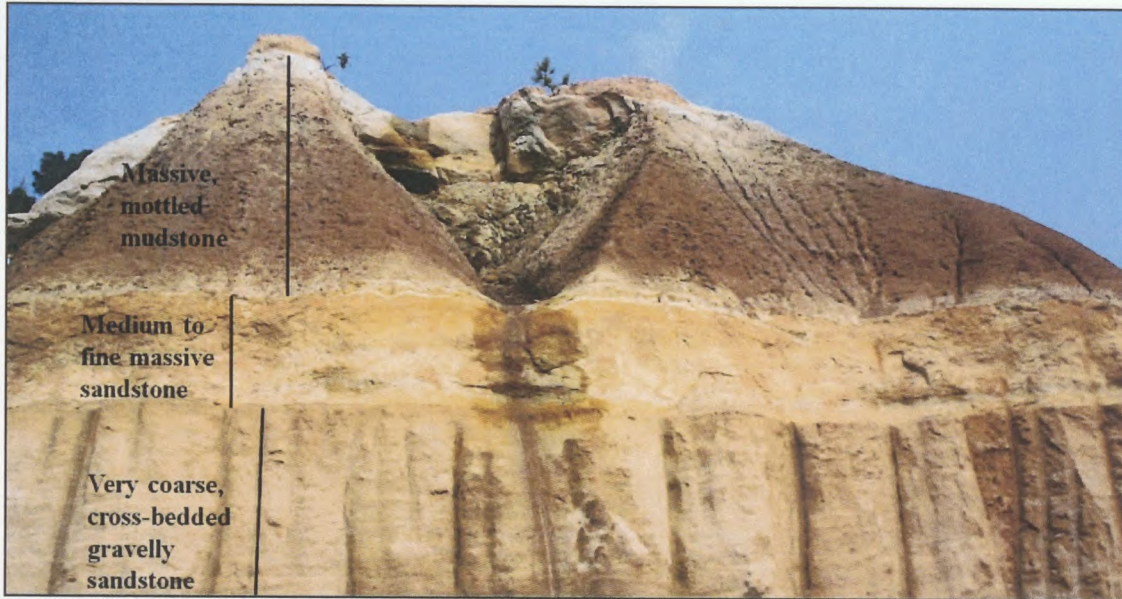


Figure 30: Station DB102. Tuscaloosa outcrop in Phenix City, AL showing an overall fining upward sequence (Image courtesy of Dr. Bill Frazier).

Station DB102 demonstrates the fining upward nature of the Tuscaloosa Formation sedimentary sequence. The outcrop measures approximately 400 ft (122 m) horizontally from north to south and vertically ranges from approximately 20 ft (6.1 m) to greater than 50 ft (15.2 m) in thickness and is divided into three distinct layers. The lower unit consists of a conglomerate containing coarse, dark red and dark yellow pisoliths in addition to locally derived gneiss pebbles. The middle unit consists of medium to fine-grained massive sandstone, while the upper layer is a highly mottled mudstone.

A comparison of the grain size of the lower and middle units shows a distinct decline in grain size of the middle layer compared to the lower layer (Figs. 32, 33).

Figure 30: DB102 Tuscaloosa Formation outcrop showing an overall fining upward sequence (Image courtesy of Dr. Bill Frazier).

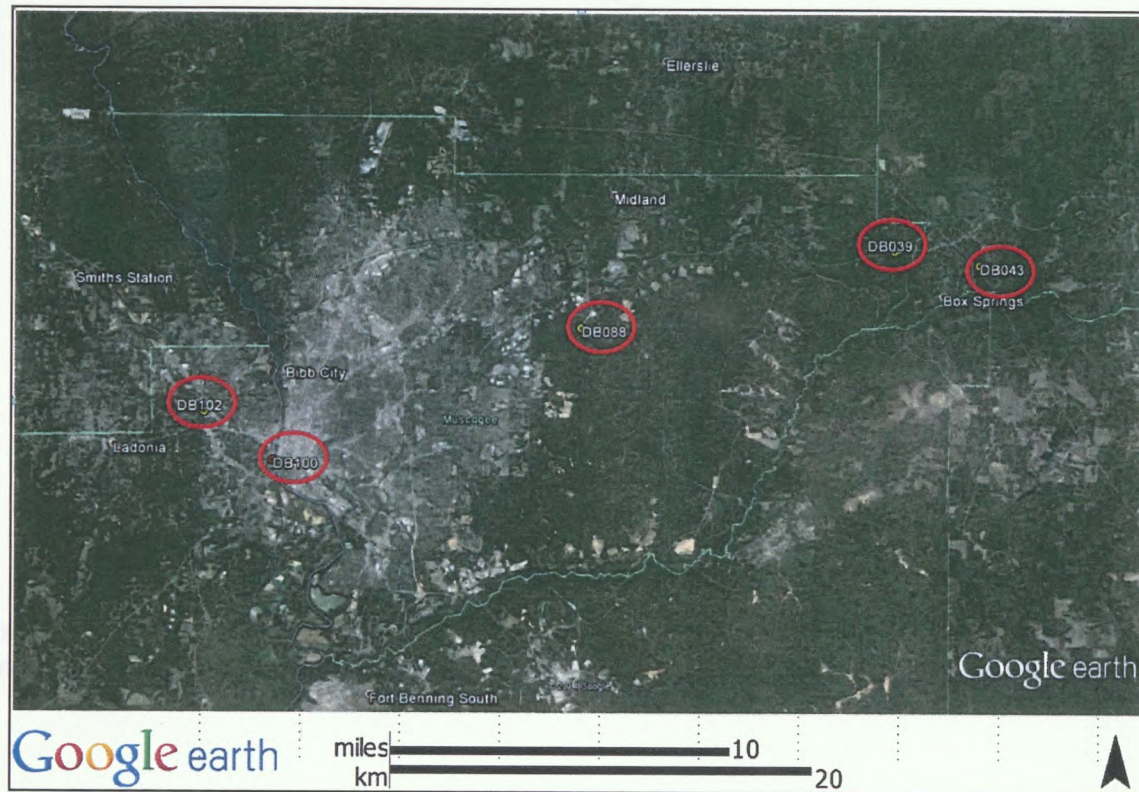


Figure 31: Location of samples used for grain size analysis.

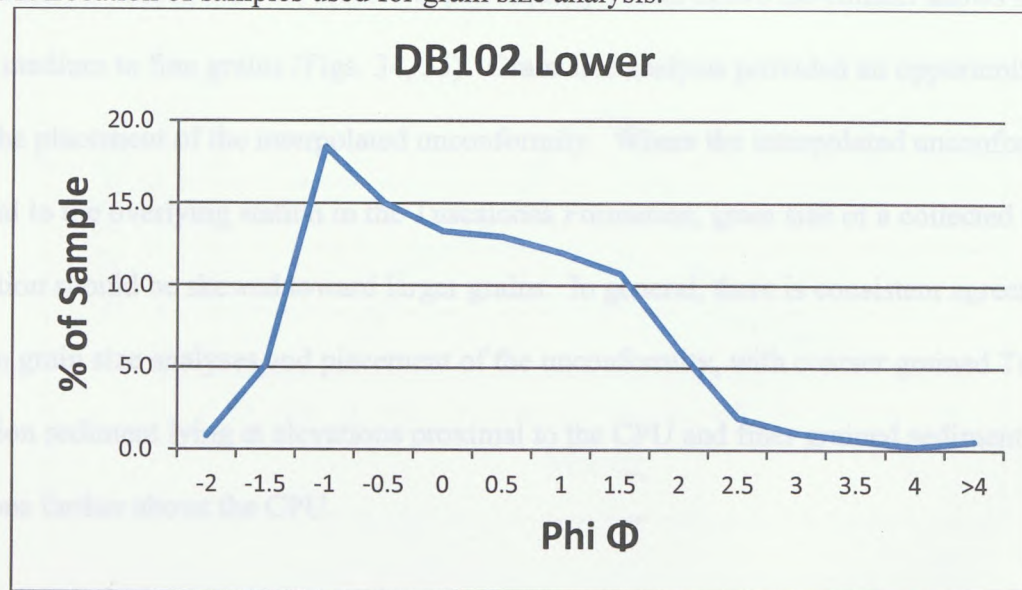


Figure 32: DB102 Basal Tuscaloosa Formation sediment is dominated by coarse, gravelly sandstone.

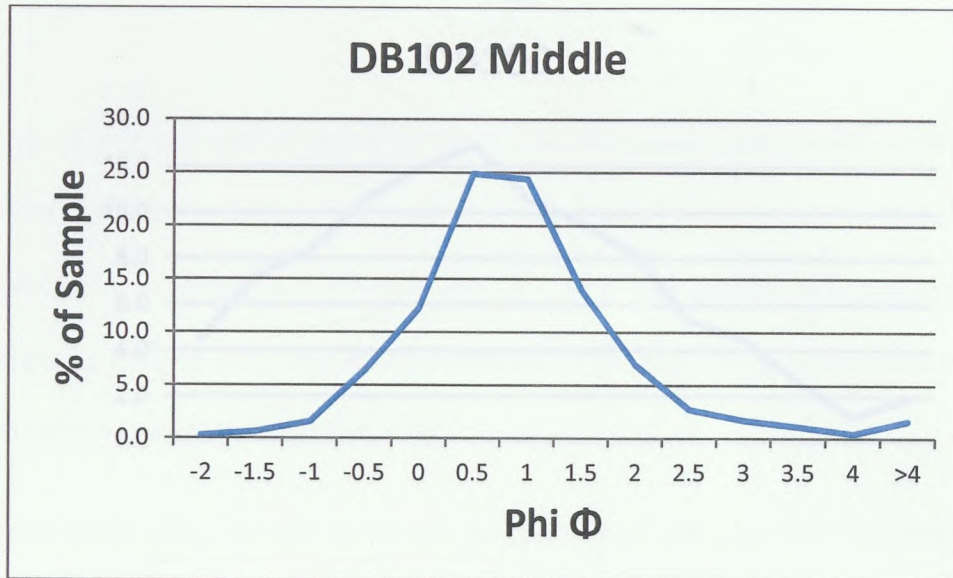


Figure 33: DB102 Sediment from the middle of the Tuscaloosa Formation is dominated by medium to fine-grained massive sandstone.

Station DB100, which is located directly at an observable contact, shows skewness toward larger grains, whereas station DB088, located approximately 11.6m above the contact shows skewness toward medium to fine grains (Figs. 34, 35). Grain size analysis provided an opportunity to check the placement of the interpolated unconformity. Where the interpolated unconformity was proximal to the overlying station in the Tuscaloosa Formation, grain size of a collected sample at that station should be skewed toward larger grains. In general, there is consistent agreement between grain size analyses and placement of the unconformity, with coarser grained Tuscaloosa Formation sediment lying at elevations proximal to the CPU and finer grained sediment lying at elevations farther above the CPU.

Figure 34: Station located ~11.6m above the CPU contact skewed toward finer grains.

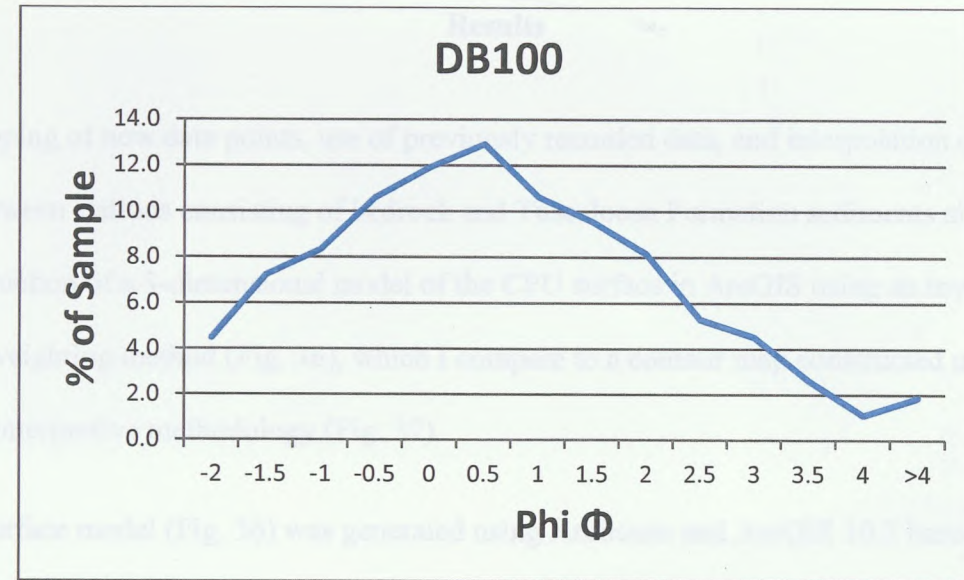


Figure 34: DB100 located at observable contact with basement skewed toward larger grains.

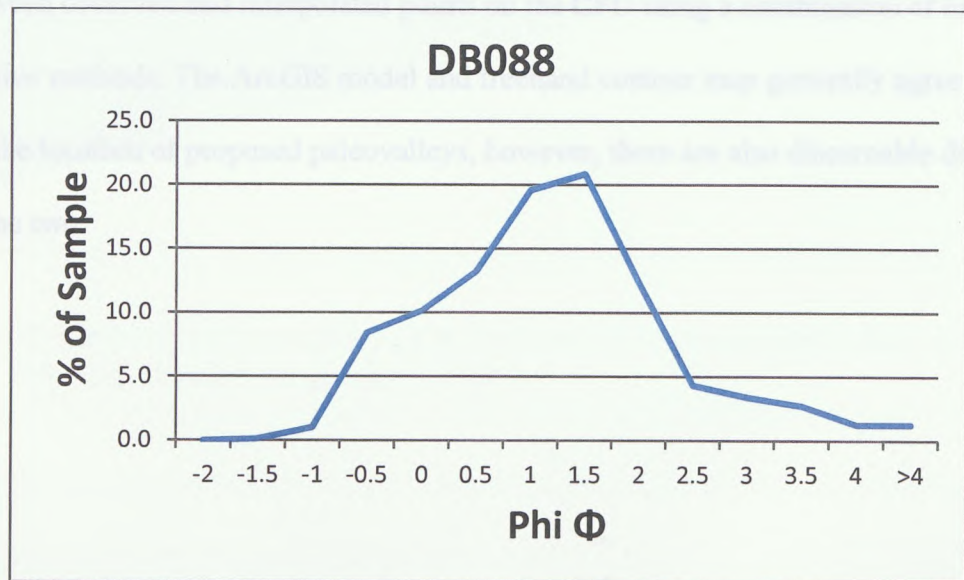


Figure 35: DB088 located ~11.6 m above the CPU contact skewed toward finer grains.

Results

Field mapping of new data points, use of previously recorded data, and interpolation of data points between stations consisting of bedrock and Tuscaloosa Formation sediments allowed for the construction of a 3-dimensional model of the CPU surface in ArcGIS using an inverse distance weighting method (Fig. 36), which I compare to a contour map constructed using a freehand interpretive methodology (Fig. 37).

The 3D surface model (Fig. 36) was generated using ArcScene and ArcGIS 10.2 based on coordinates of observed and interpolated contacts. A 13:1 vertical exaggeration was necessary to view the model three dimensionally due to the relatively low relief compared to the longitudinal scale of the study area. In contrast, the freehand interpretive contour map was drawn in Google Earth between observed and interpolated points on the CPU using a combination of interpretive and objective methods. The ArcGIS model and freehand contour map generally agree with regard to the location of proposed paleovalleys, however, there are also discernable discrepancies between the two.

Figure 36: 3D surface of contact surface produced in ArcGIS using available data. Contour interval is 700 (3m). Vertical exaggeration is 13:1.

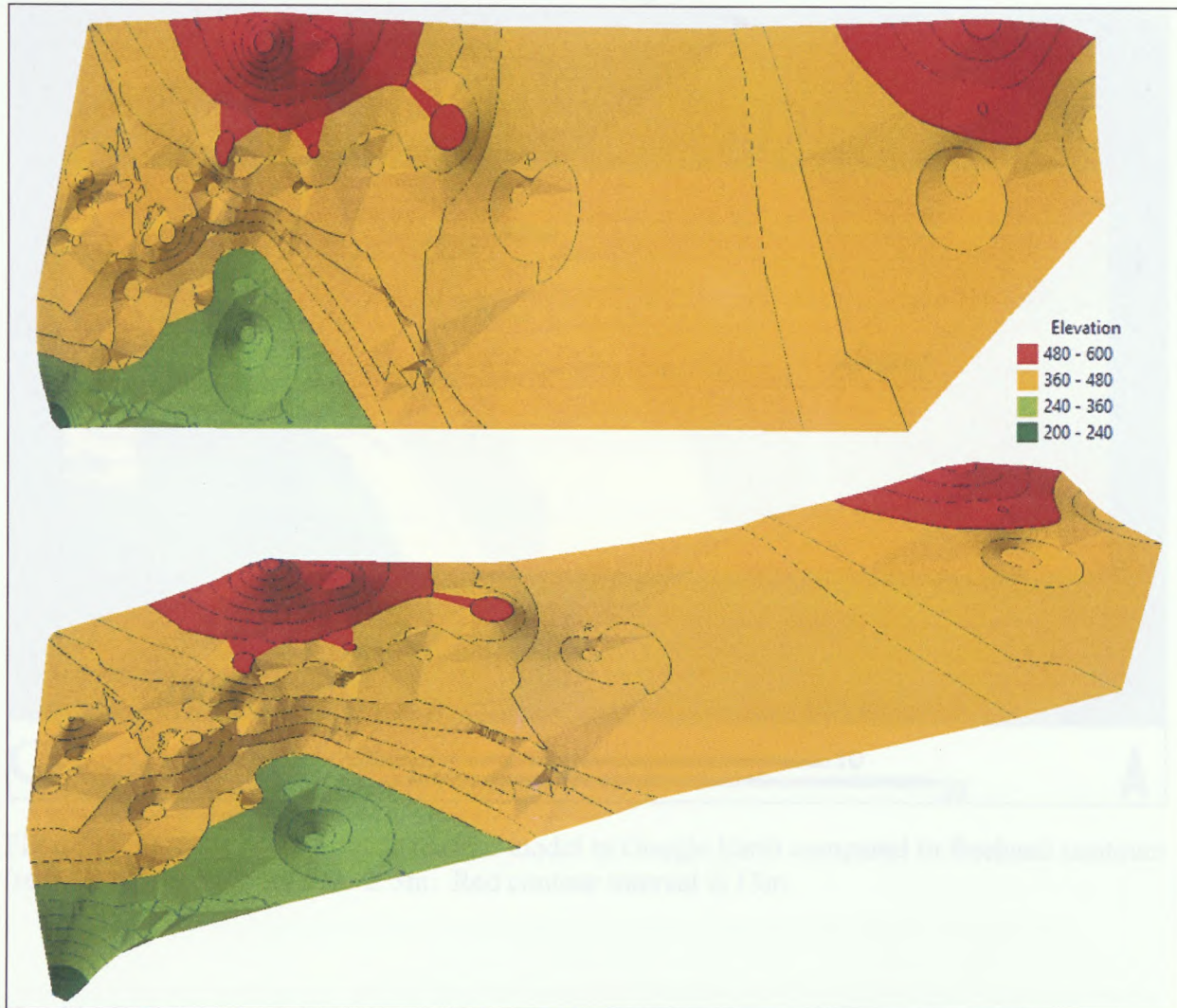


Figure 36: 3D surface of contact surface produced in ArcGIS using available data. Contour interval is 10ft (3m). Vertical exaggeration is 13:1.

portion of the surface is shown in the 3D contact model in Figure 36. The model 'bumps' seen are the result of the tracings on which surfaces the computer generated surface processes. Raster datasets, particularly which stations at that points are separated by large distances with sparse data. In this case, the closed contours lines recorded along the ArcGIS surface (ridges and depressions) may be produced by the contouring algorithm when such features would not be created during band contouring. It is therefore more likely that the band contoured map is more representative of the actual CFS surface. Future mapping methodologies

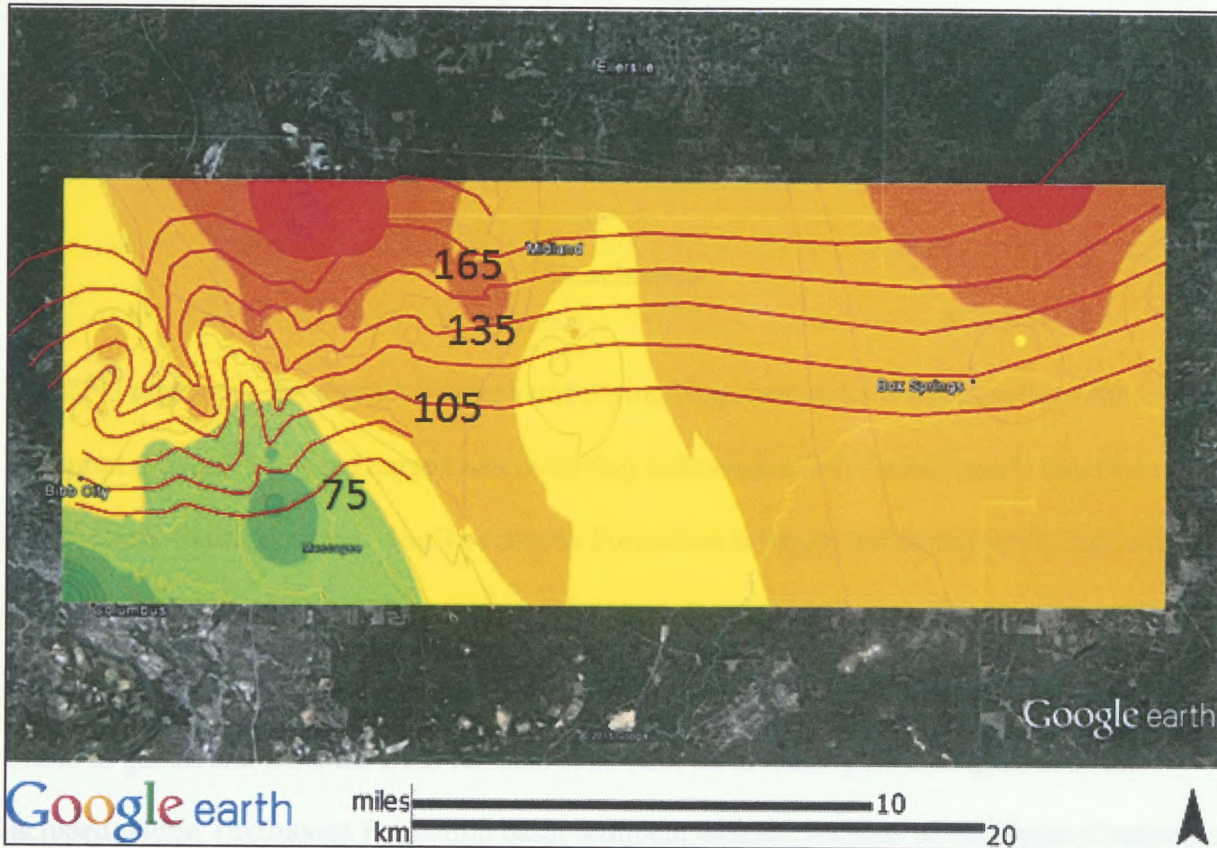


Figure 37: Overlay of the contact surface model in Google Earth compared to freehand contours (red). Black contour interval is 3m. Red contour interval is 15m.

Notable difference include a series of closed contours indicating prominent hills and depressions in the GIS model, which are notably absent in the freehand contours. Additionally, the prominence of the western-most channel in the freehand contours is diminished in the GIS model. Such variances are the result of the manner in which software for computer-generated surfaces processes limited datasets, particularly when clusters of data points are separated by large distances with sparse data. In this case, the closed contour lines scattered across the ArcGIS surface (hills and depressions) may be produced by the contouring algorithms when such features would not be created during hand contouring. It is therefore more likely that the hand contoured map is more representative of the actual CPU surface. Future mapping work should

increase the number of data points available and improve the accuracy of the CPU surface in the study area.

Several independent sources were corroborated on limited outcrop exposures. Similar relief patterns on both the basement upper surface and sedimentary lower surface independent of the interpolated data. Third, modern analogs in southeastern Brazil have similar relief to the inferred paleotopography of the LCRV and were used to estimate

Conclusions

The CPU represents the contact between underlying basement rocks/residual soils of the western Piedmont province's Uchee terrane and overlying sediments of the Tuscaloosa Formation of the Gulf Coastal Plain province. The Tuscaloosa Formation is the lowest stratigraphic unit within

the Coastal Plain in the LCRV of western Georgia and eastern Alabama. Earliest deposition of Tuscaloosa sediments began ~100 Ma in the Cenomanian and ended ~80 Ma in the Santonian.

Clasts of gneiss and pisoliths from residual soils built on metamorphic and igneous rocks included within Tuscaloosa Formation basal sediment indicate incision of the Upper Cretaceous surface into the underlying saprolitic basement. This strongly indicates the CPU in the vicinity of the LCRV is located within the Tuscaloosa Formation, between the basal paleosol and overlying fluvial sediments, rather than between the Tuscaloosa Formation and basement rocks of the Uchee terrane.

Mapping of the contact between the basement-paleosol and Tuscaloosa Formation sediments within the LCRV is difficult due to urban development, but limited exposures on the CPU can be used in conjunction with interpolated points on the CPU derived from available exposures of basement, paleosol and sedimentary sequences to create a paleotopographic surface representing the Upper Cretaceous surface. The accuracy of the interpolation method used here can be validated through a number of independent checks. First, interpolation of the CPU between observed outcrop of basement and sedimentary units produced multiple data clusters which

showed consistent elevation values and consistent topographic gradients between independent data points. Second, independent contour maps constructed on basement and sediment exposures indicate similar relief patterns on both the basement upper surface and sedimentary lower surface independent of the interpolated data. Third, modern analogs in southeastern Brazil have similar relief to the inferred paleotopography of the CPU and were used to estimate potential error in the interpolated surface. Results indicate interpolated elevation data is within $\pm 1.0\text{m}$ to $\pm 3.4\text{m}$ of the location of the CPU for stations within 122m to 579m of one another. Finally, sedimentary analysis used to constrain the stratigraphic position of collected samples within the Tuscaloosa Formation yield results consistent with the interpolated position of the CPU.

Previous research by Frazier and Taylor (1980) indicates the younger Eutaw Formation, disconformably overlying the Tuscaloosa Formation, is comprised entirely of marine sediments deposited in a near-shore estuary environment and indicates a marine transgression following deposition of fluvial sequences in the Tuscaloosa Formation. Research by Osborne (2013) indicates sediments of the Eutaw Formation sourced differing provenances, with sediments in western Georgia likely sourcing the Pine Mountain area. Heavy minerals in Eutaw Formation sediment may indicate a more mineralogically diverse source than that of the Tuscaloosa Formation, which consists predominately of quartz in a kaolin matrix. Alternatively, heavy mineral assemblages in the Eutaw Formation suggest less intense chemical weathering during deposition of the Eutaw Formation. Regardless, this mineralogical diversity implies that Eutaw Formation sediments are not derived from recycling of Tuscaloosa Formation sediments, but rather were sourced from highlands beyond the extent of the Tuscaloosa. This data, coupled with the presence of similarly located paleovalleys identified in both the Tuscaloosa and Eutaw

Formations, indicates that the drainage system responsible for deposition of Tuscaloosa

Formation sediments persisted from the Cenomanian into the Campanian (10.3-28.4 m.y.).

Presented at 2013 Southeastern Geological Society of America, Roanoke, VA.

Bishay, R.C., 2013, Early Cenozoic Environment—105 Ma / 710–1001 (Cenozoic Stage), Retrieved April 15, 2015 from <http://www.sedulog.org/2013/04/01/early-cenozoic-environment-105-ma-710-1001-cenozoic-stage/>

Cohen, K.M., Finney, S.C., Gibbons, P.R., and Haas, J.-X., 2013, The IUGS International Chronostratigraphic Chart: Episodes, v. 36, no. 3, p. 199–204.

Dennett, C.W., 1953, Nomenclature of Outcropping Tuscaloosa Group in Alabama, American Association of Petroleum Geologists Bulletin, v. 37, no. 3, p. 525–538.

Ehrhart, D.H., 1955, Stratigraphy of the Outcropping Cenozoic Rocks of Georgia, Geological Survey Bulletin 1014, p. 74.

Frazier, W.J., 1996, Facies Deposits in the Cutler and Shallowater Formations (Bentonian and Coniacian) of Southwestern Georgia and Adjacent Alabama and their Stratigraphic Significance, Geological Society of America, Abstracts with Programs, 1996, v. 12.

Frazier, W.J., Hadley, T.B., and Schmitzner, D.R., 1997, Geology of the Fall Line: A field guide to the structure and petrology of the Uchee Belt and facies stratigraphy of the Lower Formation in southwestern Georgia and adjacent Alabama, Georgia Geological Society, 22nd Annual Field Trip, p. 81–92.

Frazier, W.J., and Taylor, R.S., 1998, Facies Changes and Palaeogeographic Interpretations of the Lower Formation (Upper Cenomanian) from Western Georgia to Central Alabama, p. 1–27

Frazier, W.J., Hadley, T.B., and Schmitzner, D.R., 1997, Geology of the Fall Line: A field guide to the structure and petrology of the Uchee Belt and facies stratigraphy of the Lower Formation in southwestern Georgia and adjacent Alabama, Georgia Geological Society 22nd Annual Field Trip, p. 81–92.

Hadley, T.B., and Scheepers, M.G., 1997, Mylonites and other fault-related rocks of the Pine Mountain and Uchee belts in western Alabama and western Georgia, Southeastern Section of the Geological Society of America Field Trip Guidebook, 1997.

Martin, W.H., and Crimell, M.S., 1971, A guide to selected upper Cenomanian and lower Santonian outcrops in the lower Chattahoochee River valley of Georgia, Guidebook 15, Georgia Geological Survey, p. 1–6.

Mohammed, N.Z., Ghazi, A., and Mustafa, H.M., 2013, Positional Accuracy Testing of Google Earth, International Journal of Multidisciplinary Sciences and Engineering, v. 4, no. 6, p. 6–9.

Works Cited

- Black, D.L., Osborne, D., Barineau, C., and Frazier, W., 2014, Long-lived Upper Cretaceous Paleodrainage System in the U.S. Southwestern Georgia-Southeastern Alabama Region, Poster presented at 2014 Southeastern Geological Society of America, Blacksburg, VA
- Blakey, R.C., 2013, Early (“Mid”) Cretaceous—105 Ma (110-100) [Online image]. Retrieved April 15, 2015 from http://cpgeosystems.com/images/NAM_key-105Ma_EarK-sm.jpg
- Cohen, K.M., Finney, S.C., Gibbard, P.L., and Fan, J.-X., 2013, The ICS International Chronostratigraphic Chart: Episodes, v. 36, no. 3, p. 199–204.
- Drennen, C.W., 1953, Reclassification of Outcropping Tuscaloosa Group in Alabama. American Association of Petroleum Geologists Bulletin, v. 37, no. 3, p. 522-538.
- Eargle, D.H., 1955, Stratigraphy of the Outcropping Cretaceous Rocks of Georgia. Geological Survey Bulletin 1014, p. 7-8.
- Frazier, W.J., 1996, Estuarine Deposits in the Eutaw and Blufftown Formations (Santonian and Campanian) of Southwestern Georgia and adjacent Alabama and their Sequence-Stratigraphic Significance. Geological Society of America, Abstracts with Programs, 28(2):12
- Frazier, W.J., Hanley, T.B., and Schwimmer, D.R., 1987, Geology of the Fall Line: A field guide to the structure and petrology of the Uchee Belt and facies stratigraphy of the Eutaw Formation in southwestern Georgia and adjacent Alabama: Georgia Geological Society 22nd Annual Field Trip, p. B1-B25.
- Frazier, W.J., and Taylor, R.S., 1980, Facies Changes and Paleogeographic Interpretations of the Eutaw Formation (Upper Cretaceous) from Western Georgia to Central Alabama, p. 1-27 in Frazier, W.J., Hanley, T.B., and Schwimmer, D.R., 1987, Geology of the Fall Line: A field guide to the structure and petrology of the Uchee Belt and facies stratigraphy of the Eutaw Formation in southwestern Georgia and adjacent Alabama: Georgia Geological Society 22nd Annual Field Trip, p. B1-B25.
- Hanley, T.B., and Steltenpohl, M.G., 1997, Mylonites and other fault-related rocks of the Pine Mountain and Uchee belts of eastern Alabama and western Georgia: Southeastern Section of the Geological Society of America Field Trip Guidebook, 78 p.
- Marsalis, W.E. and Friddell, M.S., 1975, A guide to selected upper Cretaceous and lower tertiary outcrops in the lower Chattahoochee River valley of Georgia. Guidebook 15, Georgia Geological Survey, p. 1-6.
- Mohammed, N.Z., Ghazi, A., and Mustafa, H.E., 2013, Positional Accuracy Testing of Google Earth. International Journal of Multidisciplinary Sciences and Engineering, v. 4, no. 6. p. 6-9

- Monroe, W.H., Conant, L.C., and Eargle, D.H., 1946, Pre-Selma Upper Cretaceous Stratigraphy of Western Alabama. American Association of Petroleum Geologists Bulletin, v. 30, no. 2, p. 187-212.
- Osborne, D., 2013, Provenance of Detrital Sand of the Eutaw Formation in Alabama and Western Georgia: Implications for Late Cretaceous Paleogeography. Unpublished senior thesis, Columbus State University, Columbus, GA, 30 p.
- Sigleo, W., and Reinhardt, J., 1988, Paleosols from some Cretaceous environments in the southeastern United States. Geological Society of America Special Paper 216, p. 123-142.
- Smith, L.W., 1984, Depositional Setting and Stratigraphy of the Tuscaloosa Formation, Central Alabama to West-Central Georgia. Unpublished M.S. thesis, Auburn University., Auburn, AL, 125 p.
- Staheli, A.C., 1976, Topographic expression of superimposed drainage on the Georgia Piedmont, Geological Society of America Bulletin, v. 87, p. 450-452.
- Steltenpohl, M.G., Mueller, P.M., Heatherington, A.L., Hanley, T.B., and Wooden, J.L., 2008, Gondwanan/peri-Gondwanan origin for the Uchee terrane, Alabama and Georgia: Carolina zone or Suwannee terrane (?) and its suture with Grenvillian basement of the Pine Mountain window. Geosphere, 2008; v. 4; no. 1; p. 131-144; doi: 10.1130/GES00079.1.
- USGS, 1999, Map Accuracy Standards. USGS Fact Sheet 171-99.

Appendix A: Station Number, Latitude, Longitude, Elevation and Lithologic Data for Exposures of the Tuscaloosa Formation from Published and Unpublished Sources.

Name	Latitude	Longitude	Elevation (m)	Description
FT004	32.520400	-84.986000	127.1	Tuscaloosa
FT015	32.512400	-84.922500	108.5	Tuscaloosa
FT017	32.5119900	-84.901100	110.0	Tuscaloosa
FT019	32.510669	-84.892790	105.2	Tuscaloosa
FT022	32.518000	-84.886900	100.9	Tuscaloosa
FT023	32.517900	-84.876200	103.9	Tusc/Qal
FT027	32.520100	-84.918200	115.8	Tuscaloosa
FT030	32.539500	-84.933300	117.3	Igneous below Tuscaloosa
FT055	32.538300	-84.979700	142.3	Tuscaloosa
FT056	32.534274	-84.981800	114.9	Tuscaloosa above gneiss (CP unconformity)
FT067	32.548700	-84.872300	137.2	Tuscaloosa
FT076	32.523531	-84.948898	140.2	Tuscaloosa just above basement
FT091	32.577700	-84.889900	165.8	Possible Tuscaloosa
FT096	32.521800	-84.956900	128.9	Probable Tuscaloosa above gneiss
F&H, 1987	32.551725	-84.684896	140.2	Tuscaloosa above gneiss (CP unconformity)
STC003	32.505219	-84.939033	114.9	Tuscaloosa Paleosol
STC004	32.504524	-84.938194	120.7	Tuscaloosa sand
STC005	32.511920	-84.922620	109.7	Tuscaloosa Paleosol
STC006	32.522460	-84.904040	125.0	Tuscaloosa sand-gravel
STC007	32.539648	-84.898961	127.4	Tuscaloosa sand immediately above gneiss (paleovalley CP unconformity)
STC008	32.541980	-84.896030	143.0	Tuscaloosa sand
STC011	32.534570	-84.884510	123.7	Tuscaloosa Paleosol
M&F, 1975	32.482568	-84.987906	79.2	Tuscaloosa
M&F, 1975	32.484009	-84.987444	89.6	Tuscaloosa
M&F, 1975	32.506795	-84.964115	107.0	Tuscaloosa immediately above weathered gneiss (CP unconformity)
M&F, 1975	32.480834	-84.939033	90.8	Tuscaloosa sand-gravels

Appendix B: Station Number, Latitude, Longitude, Elevation and Lithologic Data for Exposures of Metamorphic and Igneous Basement from Published and Unpublished Sources.

Name	Latitude	Longitude	Elevation (m)	Description
02041204	32.602133	-84.787517	154.2	Metamorphic
02041205	32.602008	-84.787742	152.7	Metamorphic
02041902	32.614183	-84.788317	210.3	Metamorphic
02041903	32.607567	-84.787850	194.2	Metamorphic
02041904	32.603933	-84.789067	165.2	Metamorphic
02042603	32.603850	-84.789333	166.4	Metamorphic
03032501	32.705417	-84.755517	205.4	Metamorphic
03032601	32.688850	-84.782967	222.2	Metamorphic
03032602	32.686317	-84.771967	227.4	Metamorphic
03032604	32.672500	-84.751067	231.3	Metamorphic
03061001	32.552133	-85.175600	183.2	Metamorphic
03061002	32.548650	-85.176183	165.2	Metamorphic
03061003	32.549150	-85.175567	173.1	Metamorphic
03061004	32.546233	-85.178067	168.2	Metamorphic
03061005	32.551700	-85.180550	180.4	Metamorphic
03090401	32.546183	-84.937700	135.3	Metamorphic
03091301	32.534750	-84.972500	126.8	Metamorphic
03092401	32.494983	-84.994483	81.4	Metamorphic
03092402	32.444817	-84.994583	78.3	Metamorphic
03092403	32.494700	-84.994483	78.0	Metamorphic
03092404	32.496350	-84.994367	78.6	Metamorphic
04080201	32.621100	-84.802667	221.0	Metamorphic
04100301	32.550200	-84.937600	133.8	Metamorphic
04100302	32.550183	-84.936267	144.2	Metamorphic
04100303	32.550367	-84.935367	145.4	Metamorphic
04100304	32.550983	-84.934433	150.6	Metamorphic
04100305	32.550967	-84.935183	150.3	Metamorphic
04100306	32.550683	-84.936733	148.1	Metamorphic
04100307	32.550467	-84.937900	133.2	Metamorphic
05022001	32.559444	-84.956389	165.5	Metamorphic
05101001	32.681200	-84.809167	219.2	Metamorphic
05102201	32.578967	-84.902617	186.5	Metamorphic
05102202	32.572633	-84.910317	168.2	Metamorphic
05102203	32.575833	-84.900067	178.6	Metamorphic
05102205	32.592783	-84.880283	186.2	Metamorphic
07011901	32.504283	-84.993683	84.7	Metamorphic
07011902	32.502983	-84.993517	82.3	Metamorphic

Name	Latitude	Longitude	Elevation (m)	Description
07011903	32.501467	-84.994050	83.2	Metamorphic
07011904	32.507150	-84.994533	95.4	Metamorphic
07011905	32.507200	-84.995117	86.9	Metamorphic
07022401	32.559417	-84.842867	146.3	Metamorphic
07030201	32.508367	-84.937967	98.8	Metamorphic
07030301	32.557200	-84.846983	142.6	Metamorphic
07030401	32.544483	-84.868417	127.4	Metamorphic
07082201	32.599083	-84.830933	176.5	Metamorphic
08010701	32.543967	-84.935117	121.0	Metamorphic
08022502	32.534867	-84.967917	141.1	Metamorphic
08022503	32.534900	-84.968100	141.4	Metamorphic
08022504	32.534900	-84.968233	141.1	Metamorphic
08030201	32.550917	-84.935733	150.0	Metamorphic
08030202	32.550667	-84.936317	148.1	Metamorphic
08030203	32.550367	-84.937733	134.7	Metamorphic
08030204	32.550367	-84.937867	132.3	Metamorphic
08030205	32.549950	-84.937950	127.7	Metamorphic
08030206	32.549900	-84.937950	127.7	Metamorphic
08030501	32.504317	-84.993667	85.0	Metamorphic
08031001	32.525167	-84.951183	132.6	Metamorphic
08031101	32.546967	-84.884200	118.9	Metamorphic
08031102	32.546867	-84.883917	124.7	Metamorphic
08031601	32.525483	-84.951000	135.6	Metamorphic
08031602	32.525717	-84.951267	132.3	Metamorphic
08040901	32.551200	-84.926850	143.3	Metamorphic
08041801	32.540667	-84.950167	151.2	Metamorphic
08051703	32.612117	-84.808700	194.2	Metamorphic
08061101	32.582967	-84.790433	142.6	Metamorphic
08061201	32.544317	-84.882583	121.9	Metamorphic
08062301	32.545300	-84.866817	127.1	Metamorphic
08062302	32.544650	-84.883750	114.9	Metamorphic
08062601	32.547983	-84.884083	122.2	Metamorphic
08062602	32.547633	-84.883750	128.6	Metamorphic
08062701	32.546317	-84.998967	130.1	Metamorphic
08063001	32.608983	-84.993733	125.0	Metamorphic
08063002	32.608883	-84.994233	128.6	Metamorphic
08070102	32.547950	-84.885267	127.1	Metamorphic
08070103	32.548150	-84.885400	129.2	Metamorphic
08070104	32.548317	-84.885533	130.5	Metamorphic
08070701	32.611467	-84.804050	190.8	Metamorphic

Name	Latitude	Longitude	Elevation (m)	Description
08070702	32.611267	-84.804317	192.0	Metamorphic
08070703	32.610817	-84.803850	188.4	Metamorphic
08070704	32.610433	-84.803667	186.8	Metamorphic
08070705	32.609150	-84.803917	184.1	Metamorphic
08070706	32.597733	-84.813250	187.1	Metamorphic
08071001	32.549000	-84.884900	123.1	Metamorphic
08071301	32.550933	-84.934400	150.3	Metamorphic
08071302	32.544317	-84.935533	120.1	Metamorphic
08071303	32.551217	-84.926850	143.6	Metamorphic
08071701	32.537583	-84.881033	118.9	Metamorphic
08071702	32.545100	-84.884933	122.5	Metamorphic
08072201	32.610433	-84.802050	196.6	Metamorphic
08072202	32.611033	-84.802667	191.7	Metamorphic
08072203	32.610733	-84.802633	192.6	Metamorphic
08072401	32.545367	-84.991567	138.4	Metamorphic
08072402	32.545150	-84.991417	135.3	Metamorphic
08072601	32.545100	-84.990933	136.6	Metamorphic
08072602	32.545750	-84.992417	140.2	Metamorphic
08072603	32.547217	-84.991800	137.5	Metamorphic
08072604	32.546633	-84.990933	126.8	Metamorphic
08072605	32.546550	-84.990800	124.4	Metamorphic
08072606	32.546600	-84.990150	119.2	Metamorphic
08110801	32.560350	-84.932983	151.8	Metamorphic
08110802	32.559917	-84.933583	147.5	Metamorphic
09032501	32.522983	-84.991100	103.3	Metamorphic
09032502	32.521150	-84.988633	126.2	Metamorphic
09041901	32.601200	-84.829150	170.7	Metamorphic
09060701	32.515267	-85.012683	131.4	Metamorphic
09060702	32.516200	-85.016200	139.6	Metamorphic
09060901	32.518450	-85.013317	122.2	Metamorphic
09061001	32.554233	-84.913733	140.8	Metamorphic
09061002	32.554250	-84.914117	142.6	Metamorphic
09070301	32.586517	-84.944733	168.2	Metamorphic
09070501	32.640833	-84.953100	153.6	Metamorphic
09070601	32.549583	-84.967483	152.7	Metamorphic
09070801	32.560933	-84.815217	141.7	Metamorphic
09070802	32.556400	-84.813600	126.2	Metamorphic
09070803	32.556117	-84.813667	129.2	Metamorphic
09070804	32.556250	-84.813667	128.0	Metamorphic
09070805	32.552267	-84.811983	121.9	Metamorphic

Name	Latitude	Longitude	Elevation (m)	Description
09071001	32.553933	-84.812300	122.5	Metamorphic
09071002	32.554067	-84.812417	122.8	Metamorphic
09071003	32.554000	-84.812350	122.8	Metamorphic
09071004	32.552517	-84.812567	123.1	Metamorphic
09080101	32.627717	-84.946050	188.4	Metamorphic
09080102	32.610950	-84.937667	146.6	Metamorphic
09080103	32.610800	-84.938017	143.3	Metamorphic
09080104	32.611033	-84.938500	143.3	Metamorphic
09122801	32.549228	-84.980744	142.0	Metamorphic
09122802	32.545567	-84.996117	149.4	Metamorphic
09123001	32.554117	-84.980806	151.5	Metamorphic
09123002	32.554103	-84.981083	154.8	Metamorphic
10010501	32.561400	-84.953867	160.9	Metamorphic
10010504	32.558433	-84.951683	151.8	Metamorphic
10011201	32.555750	-84.976467	156.4	Metamorphic
10011301	32.540067	-84.946733	146.0	Metamorphic
10011302	32.540200	-84.947383	145.4	Metamorphic
10021401	32.555133	-84.977750	152.4	Metamorphic
10031301	32.669750	-84.913317	181.7	Metamorphic
10032301	32.599933	-84.818217	177.4	Metamorphic
10032302	32.600717	-84.818850	181.4	Metamorphic
10032601	32.669367	-84.911917	182.9	Metamorphic
10040601	32.578967	-84.973967	123.7	Metamorphic
10040602	32.578700	-84.975017	123.4	Metamorphic
10040603	32.576900	-84.979800	133.8	Metamorphic
10040604	32.559650	-84.972967	161.5	Metamorphic
10041001	32.575067	-84.983800	126.5	Metamorphic
1975111501	32.518409	-84.909073	100.9	Metamorphic
1977120701	32.514949	-84.984134	120.7	Metamorphic
1978062003	32.512829	-84.933366	101.8	Metamorphic
1978070503	32.568991	-84.905213	167.6	Metamorphic
1978071401	32.554076	-84.960158	161.5	Metamorphic
1978071403	32.575906	-84.975758	124.1	Metamorphic
1978071404	32.578618	-84.976961	121.6	Metamorphic
1978071406	32.579655	-84.976716	124.7	Metamorphic
1978072110	32.567569	-84.986029	117.0	Metamorphic
1978072902	32.572811	-84.983310	120.4	Metamorphic
1978072903	32.573702	-84.983448	118.6	Metamorphic
1978072905	32.567502	-84.986030	115.8	Metamorphic
1978073001	32.570393	-84.981710	127.7	Metamorphic

Name	Latitude	Longitude	Elevation (m)	Description
1978073002	32.570736	-84.980859	133.2	Metamorphic
1978073003	32.571233	-84.979847	143.3	Metamorphic
1978073004	32.571541	-84.979576	143.3	Metamorphic
1978073005	32.572067	-84.979011	132.3	Metamorphic
1978080901	32.610195	-84.898798	168.9	Metamorphic
1978080904A	32.607327	-84.906120	171.6	Metamorphic
1978080904B	32.607211	-84.906029	170.7	Metamorphic
1978080907	32.563311	-84.887534	138.4	Metamorphic
1978080908	32.561980	-84.887044	136.9	Metamorphic
1978080909	32.562724	-84.887628	137.2	Metamorphic
1978100401	32.543436	-84.994257	146.0	Metamorphic
1978100501	32.542245	-84.984023	139.9	Metamorphic
1978100601	32.556212	-84.983609	171.0	Metamorphic
1978100602	32.555890	-84.990013	156.1	Metamorphic
1978100603	32.556218	-84.987365	155.8	Metamorphic
1978101601	32.505653	-84.961919	106.4	Metamorphic
1978101603	32.506760	-84.962823	105.5	Metamorphic
1978102601	32.561506	-84.856134	122.5	Metamorphic
1978102701	32.554244	-84.998470	149.7	Metamorphic
1978102702	32.545662	-84.995803	147.5	Metamorphic
1978103002	32.546098	-84.884698	122.5	Metamorphic
1978103003	32.548162	-84.887267	140.5	Metamorphic
1978103004	32.548423	-84.885447	129.5	Metamorphic
1978110603	32.545323	-84.911357	116.4	Metamorphic
1978120601	32.509173	-84.936070	101.2	Metamorphic
1978123101A	32.610409	-84.913253	163.4	Metamorphic
1978123101B	32.609970	-84.912080	166.1	Metamorphic
1979011906	32.513195	-84.987210	111.6	Metamorphic
1979012201	32.512798	-84.986608	107.9	Metamorphic
1979012202	32.512398	-84.986438	106.1	Metamorphic
1979012203	32.511957	-84.986318	98.8	Metamorphic
1979021501A	32.541585	-84.995924	138.7	Metamorphic
1979021501B	32.541356	-84.995354	134.1	Metamorphic
1979022602	32.554104	-84.998538	148.4	Metamorphic
1980022205	32.552377	-84.990653	135.0	Metamorphic
1980022206	32.552987	-84.990640	141.4	Metamorphic
1980022601	32.528468	-84.963819	137.5	Metamorphic
1980022801	32.528918	-84.957304	136.2	Metamorphic
1980022802	32.527904	-84.957834	134.1	Metamorphic
1980030901	32.530440	-84.984320	134.4	Metamorphic

Name	Latitude	Longitude	Elevation (m)	Description
1980030902	32.532342	-84.987501	134.7	Metamorphic
1980030903	32.531618	-84.987318	130.5	Metamorphic
1980030908A	32.552158	-84.966930	149.4	Metamorphic
1980030908B	32.551881	-84.967086	148.1	Metamorphic
1980040701	32.539892	-84.960907	132.0	Metamorphic
1980041401	32.532108	-84.970127	128.3	Metamorphic
1980041501	32.522822	-84.935592	106.7	Metamorphic
1980041901	32.536413	-84.946969	130.1	Metamorphic
1980041902	32.533901	-84.947026	126.8	Metamorphic
1980042101	32.534362	-84.967491	139.0	Metamorphic
1980042501	32.537632	-84.955717	142.0	Metamorphic
1980050103	32.518671	-84.956993	120.7	Metamorphic
1980050104	32.520214	-84.989308	121.6	Metamorphic
1980050106	32.511031	-84.994114	96.3	Metamorphic
1980050108	32.513614	-84.990191	114.0	Metamorphic
1980050501	32.532326	-84.969787	130.5	Metamorphic
1980050502	32.541928	-84.931748	120.1	Metamorphic
1980050503	32.547977	-84.921077	123.7	Metamorphic
1980050601	32.527683	-84.973039	131.1	Metamorphic
1980050602	32.526562	-84.972945	128.3	Metamorphic
1980050603	32.528714	-84.974708	118.3	Metamorphic
1980051201	32.539858	-84.931750	127.4	Metamorphic
1980052301	32.540934	-84.934725	124.1	Metamorphic
1980052601	32.518314	-84.951387	114.3	Metamorphic
1980053001	32.517871	-84.940245	119.8	Metamorphic
1980060201	32.542265	-84.973671	139.0	Metamorphic
1980060202A	32.544328	-84.963950	141.1	Metamorphic
1980060202B	32.545544	-84.962336	131.4	Metamorphic
1980060202C	32.545738	-84.961875	135.3	Metamorphic
1980060202D	32.545976	-84.961673	137.5	Metamorphic
1980062101	32.547700	-84.935171	124.1	Metamorphic
1980062201	32.546085	-84.928163	145.4	Metamorphic
1980072801	32.553623	-84.981155	156.7	Metamorphic
1980080102	32.554431	-84.854563	139.0	Metamorphic
1980080103	32.543585	-84.869067	129.5	Metamorphic
1980080701	32.554016	-84.854461	139.0	Metamorphic
1980080702	32.554015	-84.854381	138.7	Metamorphic
1980080703	32.558563	-84.842807	153.0	Metamorphic
1980080704	32.569190	-84.827090	161.5	Metamorphic
1980080705	32.568333	-84.879526	161.5	Metamorphic

Name	Latitude	Longitude	Elevation (m)	Description
1980081501	32.547721	-84.946934	139.6	Metamorphic
1980081503	32.548183	-84.951267	149.7	Metamorphic
1980082005	32.561285	-84.953719	160.3	Metamorphic
1980082006	32.561545	-84.952341	163.1	Metamorphic
1980090401	32.543585	-84.936052	132.0	Metamorphic
1980090801	32.554000	-84.981403	155.1	Metamorphic
1980090802	32.553623	-84.981155	156.7	Metamorphic
1980090901	32.530129	-84.985375	128.6	Metamorphic
1980090902	32.530573	-84.982737	129.8	Metamorphic
1980091001A	32.572735	-84.864417	161.8	Metamorphic
1980091001B	32.573014	-84.864515	163.4	Metamorphic
1980091001C	32.573415	-84.864495	163.7	Metamorphic
1980091901	32.549697	-84.882889	138.7	Metamorphic
1980092401	32.577525	-84.820425	157.9	Metamorphic
1980092402	32.572680	-84.824207	160.9	Metamorphic
1980092601	32.520378	-84.987846	123.1	Metamorphic
1980092701	32.539552	-84.899535	126.8	Metamorphic
1980092703	32.531131	-84.878611	103.9	Metamorphic
1980102903	32.522620	-84.989607	119.8	Metamorphic
1980102904	32.522145	-84.988872	114.9	Metamorphic
1980121502	32.521929	-84.985403	133.5	Metamorphic
1980121601	32.543762	-84.993476	135.3	Metamorphic
1980121602	32.539363	-84.995446	129.8	Metamorphic
1980121603	32.524808	-84.978939	125.0	Metamorphic
1980121604	32.525044	-84.979821	122.5	Metamorphic
1980121703	32.528161	-84.931404	117.0	Metamorphic
1980122801	32.540755	-84.955239	145.7	Metamorphic
1980122802	32.539702	-84.954963	144.2	Metamorphic
1980122803	32.530732	-84.982059	120.1	Metamorphic
1980123004	32.517986	-84.992339	105.8	Metamorphic
1980123005	32.519080	-84.994485	102.4	Metamorphic
1980123006	32.518677	-84.996094	102.4	Metamorphic
1980123007	32.518452	-84.996321	102.4	Metamorphic
1981011803	32.516877	-84.978398	110.0	Metamorphic
1981020101	32.553410	-84.996175	140.2	Metamorphic
1981020102	32.554104	-84.998538	148.4	Metamorphic
1981020103	32.548310	-84.994944	149.0	Metamorphic
1981020104	32.547456	-84.995228	146.6	Metamorphic
1981020105	32.550220	-84.995882	140.2	Metamorphic
1981030701	32.531092	-84.992657	116.1	Metamorphic

Name	Latitude	Longitude	Elevation (m)	Description
1981032901	32.534297	-84.973780	132.0	Metamorphic
1981040301	32.507287	-84.994792	95.1	Metamorphic
1981040501	32.530024	-84.974127	130.5	Metamorphic
1981040502	32.528875	-84.976165	128.0	Metamorphic
1981040503	32.526837	-84.977003	125.0	Metamorphic
1981040505	32.528465	-84.976272	128.6	Metamorphic
1981041005	32.547971	-84.908687	133.8	Metamorphic
1981041006	32.545183	-84.911425	117.7	Metamorphic
1981041201	32.526689	-84.979435	116.4	Metamorphic
1981041202	32.524242	-84.979753	122.2	Metamorphic
1981041203	32.525279	-84.981607	122.5	Metamorphic
1981041703	32.532899	-84.851838	113.4	Metamorphic
1981041705	32.540465	-84.824494	122.8	Metamorphic
1981042001	32.538230	-84.901099	118.0	Metamorphic
1981042401	32.557298	-84.903235	135.0	Metamorphic
1981042402	32.558356	-84.903890	139.0	Metamorphic
1981042403	32.556641	-84.903122	133.5	Metamorphic
1981042404	32.554323	-84.903196	129.5	Metamorphic
1981042405	32.563981	-84.900632	160.9	Metamorphic
1981042406	32.555545	-84.897803	157.6	Metamorphic
1981042602	32.527177	-84.975162	124.7	Metamorphic
1981042701	32.565140	-84.955462	169.2	Metamorphic
1981050501	32.551263	-84.926600	144.8	Metamorphic
1981051801	32.542269	-84.927611	139.0	Metamorphic
1981060702	32.522585	-84.991326	107.6	Metamorphic
1981060705	32.520029	-84.992040	106.1	Metamorphic
1981060706	32.557720	-84.943456	153.9	Metamorphic
1981060707	32.557255	-84.943431	156.1	Metamorphic
1981060708	32.558009	-84.943208	151.8	Metamorphic
1981061704	32.514614	-84.995711	80.8	Metamorphic
1981070501	32.517748	-84.991710	114.0	Metamorphic
1981070503	32.525236	-84.980869	117.0	Metamorphic
1981071301	32.542478	-84.913421	115.2	Metamorphic
1981071302	32.544939	-84.909359	132.6	Metamorphic
1981072601	32.571914	-84.903211	171.6	Metamorphic
1981072602	32.581220	-84.902869	181.1	Metamorphic
1981122901	32.599785	-84.879070	201.5	Metamorphic
1981122902	32.600027	-84.891909	198.7	Metamorphic
1981123002	32.597008	-84.897651	206.3	Metamorphic
1981123004	32.582149	-84.911108	185.3	Metamorphic

Name	Latitude	Longitude	Elevation (m)	Description
1981123005	32.556414	-84.961529	161.8	Metamorphic
1982010802	32.619305	-84.811040	214.3	Metamorphic
1982070803	32.595590	-84.792208	172.2	Metamorphic
1982010804	32.593611	-84.790017	171.3	Metamorphic
1982010805	32.599738	-84.795183	184.1	Metamorphic
1982010806	32.612175	-84.799018	206.7	Metamorphic
1982010807	32.613893	-84.800013	213.1	Metamorphic
1982011502	32.538479	-84.844600	118.9	Metamorphic
1982011503	32.538406	-84.846973	116.4	Metamorphic
1982011504	32.538769	-84.848380	106.4	Metamorphic
1982011505	32.545918	-84.866569	129.5	Metamorphic
1982012001	32.550502	-84.961551	141.7	Metamorphic
1982013101	32.562846	-84.962977	151.8	Metamorphic
1982013102	32.562829	-84.962770	152.1	Metamorphic
1982013103	32.568248	-84.961554	163.1	Metamorphic
1982013105	32.578528	-84.961440	137.8	Metamorphic
1982013106	32.579646	-84.960647	131.4	Metamorphic
1982020102	32.586332	-84.944785	167.6	Metamorphic
1982020103	32.591368	-84.941394	165.8	Metamorphic
1982020104	32.594473	-84.947570	169.8	Metamorphic
1982020105	32.601565	-84.948637	153.6	Metamorphic
1982020106	32.602289	-84.949064	147.8	Metamorphic
1982020108	32.616924	-84.939535	174.0	Metamorphic
1982020109	32.623073	-84.942350	193.9	Metamorphic
1982020110	32.623992	-84.942525	196.0	Metamorphic
1982020401	32.589647	-84.958098	151.2	Metamorphic
1982020403	32.590921	-84.957286	151.5	Metamorphic
1982020702	32.613093	-84.950066	179.5	Metamorphic
1982022801	32.532555	-84.964859	124.1	Metamorphic
1982022802	32.533036	-84.964660	124.1	Metamorphic
1982031501	32.552212	-84.905730	154.5	Metamorphic
1982031502	32.551555	-84.908840	146.9	Metamorphic
1982042201	32.522171	-84.983744	138.1	Metamorphic
1982042202	32.522812	-84.983915	136.6	Metamorphic
1982042204	32.524126	-84.978692	125.6	Metamorphic
1982092002	32.534884	-84.848787	106.4	Metamorphic
1982092003	32.537173	-84.848705	105.2	Metamorphic
1982092005	32.539282	-84.848775	108.5	Metamorphic
1982101801	32.529455	-84.910518	109.4	Metamorphic
1982101802	32.532202	-84.909932	110.3	Metamorphic

Name	Latitude	Longitude	Elevation (m)	Description
1982101901	32.542379	-84.912150	112.8	Metamorphic
1982101905	32.547292	-84.913221	129.5	Metamorphic
1983062606	32.553223	-84.936488	148.7	Metamorphic
1984032401	32.610463	-84.937732	143.9	Metamorphic
1984032402	32.623169	-84.946898	193.9	Metamorphic
1984032403	32.621904	-84.946166	187.8	Metamorphic
1984032404	32.617580	-84.943491	165.5	Metamorphic
1984040101	32.504691	-84.990019	101.2	Metamorphic
1984040102	32.504269	-84.989498	95.4	Metamorphic
1984040103	32.550666	-84.949704	152.4	Metamorphic
1985021701	32.541088	-84.962895	130.1	Metamorphic
1985041901	32.586355	-84.948855	163.1	Metamorphic
1985052701	32.574648	-84.976167	137.2	Metamorphic
1985052702	32.574948	-84.975144	129.5	Metamorphic
1985052703	32.584977	-84.976767	154.2	Metamorphic
1985052705	32.623599	-84.991785	154.8	Metamorphic
1985062401	32.529287	-84.849835	100.0	Metamorphic
1985062402	32.528247	-84.849197	99.1	Metamorphic
1985112301	32.543274	-84.935938	132.3	Metamorphic
1986010301	32.541334	-84.870963	128.6	Metamorphic
1986011401	32.582526	-84.752756	165.5	Metamorphic
1987030101	32.554152	-84.897290	152.1	Metamorphic
1987030202	32.567593	-84.907139	146.0	Metamorphic
1987030203	32.546749	-84.884017	121.6	Metamorphic
1987030204	32.538031	-84.880658	123.1	Metamorphic
1987030301	32.539088	-84.971463	130.1	Metamorphic
1987050502	32.538265	-84.880853	123.1	Metamorphic
1987052501	32.580880	-84.906967	181.4	Metamorphic
1987052502	32.583090	-84.910160	185.9	Metamorphic
1988053001	32.536136	-84.990488	112.8	Metamorphic
1988121301	32.536906	-84.995075	134.7	Metamorphic
1988121305	32.536123	-84.995278	138.7	Metamorphic
1989011401	32.515526	-84.952654	109.4	Metamorphic
1990022801	32.555784	-84.927056	131.7	Metamorphic
1990022802	32.566587	-84.935731	175.6	Metamorphic
1990073101	32.543643	-84.815835	115.8	Metamorphic
1990100501	32.616092	-84.992393	133.2	Metamorphic
1990100601	32.556516	-84.972880	165.2	Metamorphic
1990101701	32.550857	-84.764574	123.7	Metamorphic
1990101702	32.550478	-84.763554	125.3	Metamorphic

Name	Latitude	Longitude	Elevation (m)	Description
1990101703	32.549517	-84.762072	123.4	Metamorphic
1990101704	32.548825	-84.763771	123.7	Metamorphic
1991022701	32.608594	-84.876029	220.1	Metamorphic
1991032701	32.605931	-84.876292	210.9	Metamorphic
1991032702	32.606293	-84.876936	210.6	Metamorphic
1991032703	32.605453	-84.875443	211.2	Metamorphic
1991032705	32.605330	-84.873958	214.6	Metamorphic
1991032706	32.605376	-84.873044	214.3	Metamorphic
1992102601	32.543939	-84.889690	124.4	Metamorphic
1992112701	32.541189	-84.898530	139.9	Metamorphic
1992112702	32.543777	-84.902333	118.6	Metamorphic
1992112703	32.541343	-84.897141	142.3	Metamorphic
1992112704	32.540662	-84.898921	139.9	Metamorphic
1992121401	32.551788	-84.897148	153.0	Metamorphic
1993120701	32.597360	-84.793254	182.0	Metamorphic
1993120703	32.591144	-84.820332	177.1	Metamorphic
1996080101	32.616433	-84.850996	199.0	Metamorphic
1996080102	32.616388	-84.849431	206.0	Metamorphic
1996080103	32.616257	-84.847747	216.4	Metamorphic
1996080103	32.616257	-84.847747	216.4	Metamorphic
1996080105	32.615995	-84.847314	219.2	Metamorphic
1996080106	32.615755	-84.846950	219.8	Metamorphic
1996080202	32.601493	-84.832075	189.6	Metamorphic
1996080203	32.599696	-84.831215	179.8	Metamorphic
1996080204	32.600020	-84.830537	178.3	Metamorphic
1996080205	32.601139	-84.829107	170.7	Metamorphic
1996080206	32.601378	-84.828979	172.5	Metamorphic
1996080207	32.601824	-84.828828	175.3	Metamorphic
1996080208	32.615313	-84.822693	214.3	Metamorphic
1996080209	32.615499	-84.830366	222.5	Metamorphic
1996080210	32.614605	-84.833842	218.5	Metamorphic
2005101001	32.681200	-84.809200	218.8	Metamorphic
2005102202	32.572630	-84.910300	167.9	Metamorphic
2005102203	32.575830	-84.900100	178.9	Metamorphic
2005102204	32.592780	-84.880300	185.9	Metamorphic
2005122704	32.582600	-84.839200	143.9	Metamorphic
2005122705	32.582520	-84.840200	143.6	Metamorphic
2005122706	32.581650	-84.837200	157.9	Metamorphic
2005122901	32.586600	-84.834700	150.0	Metamorphic
2005122902	32.586250	-84.853530	168.6	Metamorphic

Name	Latitude	Longitude	Elevation (m)	Description
2006070302	32.569800	-85.004200	118.3	Metamorphic
2006070303	32.570830	-85.012800	105.8	Metamorphic
2006070501	32.565650	-84.999000	125.3	Metamorphic
2006070503	32.675900	-85.035100	161.8	Metamorphic
2006070701	32.570230	-85.004200	119.5	Metamorphic
2006071303	32.554180	-84.997400	144.8	Metamorphic
2006071304	32.558650	-85.002800	165.5	Metamorphic
2006071305	32.559550	-85.004100	164.9	Metamorphic
2006122602	32.550080	-84.940300	150.6	Metamorphic
2012020801	32.565030	-84.940850	167.0	Metamorphic
2012020802	32.564430	-84.941030	162.5	Metamorphic
2012020803	32.564083	-84.941483	162.5	Metamorphic
32234	32.555614	-84.930538	153.9	Metamorphic
FT001	32.507200	-84.994700	94.8	Metamorphic
FT002	32.506900	-84.994300	87.5	Metamorphic
FT003	32.524300	-84.979000	125.9	Metamorphic
FT005	32.532200	-84.879300	106.4	Metamorphic
FT006	32.531500	-84.878400	104.5	Metamorphic
FT007	32.531100	-84.878700	103.9	Metamorphic
FT009	32.544300	-84.883100	121.3	Metamorphic
FT010	32.537800	-84.880700	122.5	Metamorphic
FT011	32.537500	-84.883500	111.9	Metamorphic
FT012	32.556300	-84.911900	152.7	Metamorphic
FT014	32.558700	-84.914500	133.2	Metamorphic
FT016	32.518100	-84.909200	100.6	Metamorphic
FT018	32.520900	-84.892600	102.7	Metamorphic
FT024	32.508800	-84.878100	85.0	Metamorphic
FT025	32.507300	-84.921800	86.9	Metamorphic
FT026	32.513000	-84.933100	102.4	Metamorphic
FT028	32.522100	-84.912300	104.2	Metamorphic
FT029	32.538500	-84.932800	116.7	Metamorphic
FT031	32.568600	-84.903300	162.5	Metamorphic
FT033	32.548100	-84.908500	135.6	Metamorphic
FT034	32.546800	-84.901500	121.3	Metamorphic
FT035	32.549600	-84.887500	130.8	Metamorphic
FT036	32.583100	-84.899400	188.7	Metamorphic
FT037	32.572200	-84.911100	162.8	Metamorphic
FT041	32.499400	-84.944100	85.6	Metamorphic
FT042	32.499700	-84.944300	84.7	Metamorphic
FT043	32.500200	-84.944300	83.8	Metamorphic

Name	Latitude	Longitude	Elevation (m)	Description
FT046	32.506900	-84.941700	95.7	Metamorphic
FT047	32.506400	-84.944200	94.8	Metamorphic
FT048	32.531100	-84.964700	132.3	Metamorphic
FT049	32.536900	-84.962100	124.1	Metamorphic
FT051	32.534600	-84.964000	124.1	Metamorphic
FT052	32.533700	-84.964300	124.1	Metamorphic
FT053	32.532900	-84.964700	124.1	Metamorphic
FT054	32.531600	-84.965600	122.2	Metamorphic
FT057	32.531400	-84.981300	111.3	Metamorphic
FT059	32.563200	-84.971300	137.2	Metamorphic
FT060	32.566400	-84.956500	169.8	Metamorphic
FT061	32.565900	-84.957100	170.4	Metamorphic
FT062	32.565100	-84.946600	165.2	Metamorphic
FT063	32.556300	-85.002800	149.4	Metamorphic
FT066	32.626200	-84.996700	151.2	Metamorphic
FT068	32.552600	-84.926700	150.6	Metamorphic
FT069	32.554000	-84.926400	136.2	Metamorphic
FT073	32.551700	-84.916900	120.7	Metamorphic
FT074	32.525000	-84.951000	134.1	Metamorphic
FT077	32.531900	-84.945000	117.3	Metamorphic
FT078	32.534100	-84.946100	120.1	Metamorphic
FT079	32.542800	-84.945000	126.2	Metamorphic rock immediately below Tuscaloosa
FT080	32.561600	-84.940200	164.3	Metamorphic
FT081	32.573500	-84.921400	176.2	Metamorphic
FT082	32.572200	-84.928000	162.2	Metamorphic
FT083	32.533200	-84.902800	111.6	Metamorphic
FT086	32.536600	-84.879600	111.6	Metamorphic
FT087	32.539600	-84.899300	127.1	Metamorphic
FT088	32.542400	-84.895600	143.0	Metamorphic
FT089	32.552200	-84.873800	134.4	Metamorphic
FT092	32.581900	-84.891300	175.6	Metamorphic
FT093	32.582600	-84.902800	182.3	Metamorphic
FT094	32.581400	-84.907700	174.0	Metamorphic
FT095	32.597100	-84.903200	201.2	Metamorphic
FT096	32.521800	-84.956900	128.6	Possible Tuscaloosa above gneiss
FT097	32.582600	-84.910900	186.5	Metamorphic rock immediately below Tuscaloosa
FT100	32.596700	-84.878800	189.0	Metamorphic
FT101	32.598500	-84.879000	199.3	Metamorphic
FT102	32.589600	-84.916000	190.2	Metamorphic

Name	Latitude	Longitude	Elevation (m)	Description
FT104	32.587200	-84.926900	166.4	Metamorphic
FT107	32.583700	-84.927200	161.8	Metamorphic
FT108	32.583400	-84.927500	161.2	Metamorphic
FT109	32.582500	-84.927600	159.1	Metamorphic
FT110	32.580400	-84.927300	155.1	Metamorphic
FT111	32.575300	-84.928500	153.9	Metamorphic
FT112	32.504300	-84.993600	87.2	Metamorphic
FT113	32.512800	-84.996300	81.4	Metamorphic
FT114	32.513700	-84.995400	83.5	Metamorphic
FT115	32.513900	-84.995400	82.6	Metamorphic
FT116	32.514400	-84.995000	86.0	Metamorphic
FT117	32.514500	-84.994700	89.0	Metamorphic
STC001	32.503536	-84.944123	88.4	Gneiss
STC002	32.506851	-84.941851	95.7	Gneiss
STC009	32.548604	-84.886084	135.0	Gneiss
STC010	32.546010	-84.882160	130.1	Gneiss
STC012	32.534966	-84.882498	109.1	Gneiss

Appendix C: Station Number, Latitude, Longitude, Elevation and Lithologic Data from this Study.

Name	Latitude	Longitude	Elevation (m)	Description
DB001	32.516770	-85.011210	115.8	Metamorphic
DB002	32.516900	-85.010850	116.7	Metamorphic
DB003	32.519030	-85.011400	110.9	Metamorphic
DB004	32.519060	-85.010920	107.9	Metamorphic
DB005	32.518680	-85.011130	112.5	Metamorphic
DB006	32.518450	-85.011070	114.6	Metamorphic
DB007	32.517570	-85.013580	125.0	Tuscaloosa?
DB008	32.522410	-85.028040	149.4	Tuscaloosa?
DB009	32.523430	-85.014110	111.9	Metamorphic
DB010	32.548280	-84.926960	152.4	Metamorphic
DB011	32.538800	-85.026630	140.2	Metamorphic
DB012	32.531010	-85.047490	164.6	Tuscaloosa
DB013	32.530950	-85.047110	160.6	Tuscaloosa
DB014	32.549970	-85.034350	111.9	Metamorphic
DB015	32.549850	-85.034880	118.3	Metamorphic
DB016	32.549520	-85.035180	118.9	Metamorphic
DB017	32.552310	-85.039520	111.6	Metamorphic
DB018	32.547140	-85.040440	169.5	QAl
DB019	32.502860	-85.038510	105.2	Metamorphic
DB020	32.515970	-85.042250	139.9	Tuscaloosa
DB021	32.513460	-85.052800	122.5	Metamorphic
DB022	32.513650	-85.052830	123.1	Tuscaloosa
DB023	32.541280	-84.817690	128.9	QAl
DB024	32.547830	-84.808680	131.4	Tuscaloosa
DB026	32.545520	-84.800090	141.4	Tuscaloosa
DB027	32.542370	-84.806240	124.7	Paleosol
DB028	32.543880	-84.803630	128.0	Tuscaloosa
DB029	32.543060	-84.805100	122.2	Tuscaloosa
DB030	32.552730	-84.768150	141.4	Tuscaloosa
DB031	32.548830	-84.741970	131.4	Paleosol
DB032	32.546860	-84.732050	122.8	Paleosol
DB033	32.547130	-84.727540	124.4	Paleosol
DB034	32.545680	-84.714340	109.7	Tuscaloosa
DB035	32.546050	-84.710540	123.1	Tuscaloosa
DB036	32.548140	-84.703900	139.3	Tuscaloosa
DB037	32.547700	-84.705270	132.3	Tuscaloosa

DB038	32.564790	-84.704450	147.2	QAl
DB039	32.551730	-84.685030	139.9	Tuscaloosa
DB040	32.534790	-84.656500	111.6	Tuscaloosa
DB041	32.544990	-84.644800	120.1	Paleosol
DB042	32.545280	-84.644160	127.1	Paleosol
DB043	32.545920	-84.642560	131.4	Tuscaloosa
DB044	32.550570	-84.643490	146.6	Tuscaloosa
DB045	32.555630	-84.644380	163.4	Tuscaloosa
DB046	32.588450	-84.640710	162.2	Metamorphic
DB047	32.599140	-84.636360	172.5	Tuscaloosa
DB048	32.596170	-84.636590	168.2	Tuscaloosa
DB049	32.566230	-84.634250	158.8	Tuscaloosa
DB050	32.563810	-84.642680	153.0	Tuscaloosa
DB051	32.564410	-84.639720	146.9	Paleosol
DB052	32.562470	-84.619540	142.3	Paleosol
DB053	32.559460	-84.604580	130.8	Paleosol
DB054	32.560810	-84.604480	125.9	Metamorphic
DB055	32.547090	-84.601980	136.9	Tuscaloosa
DB056	32.518130	-84.602340	145.4	Tuscaloosa
DB057	32.502590	-84.583530	164.3	Tuscaloosa
DB058	32.511600	-84.592060	168.6	Tuscaloosa
DB059	32.574990	-84.593010	164.6	Possible bedrock, high kaolin content above
DB060	32.557320	-84.581060	158.5	Tuscaloosa
DB061	32.560730	-84.589740	133.8	Tuscaloosa
DB062	32.560960	-84.590200	131.1	Metamorphic
DB063	32.575380	-84.567050	170.1	Tuscaloosa
DB064	32.557080	-84.840030	152.1	Tuscaloosa
DB065	32.548720	-84.814920	120.4	Metamorphic
DB066	32.548210	-84.814920	120.4	Metamorphic
DB067	32.548440	-84.813480	118.6	Metamorphic
DB068	32.514480	-84.853420	105.2	Eutaw
DB069	32.528770	-84.849230	101.8	Metamorphic
DB070	32.535390	-84.848880	104.2	Metamorphic
DB071	32.526200	-84.864350	97.2	Metamorphic
DB072	32.555530	-84.874940	141.1	Metamorphic
DB073	32.555690	-84.875080	142.3	Paleosol
DB074	32.554890	-84.875600	141.1	Contact
DB075	32.554760	-84.875270	140.2	Metamorphic
DB076	32.554930	-84.873820	139.3	Metamorphic
DB077	32.539340	-84.812910	110.0	Metamorphic
DB078	32.539590	-84.812840	110.0	Metamorphic

DB079	32.536710	-84.816730	124.7	Tuscaloosa sand
DB080	32.592150	-84.637210	167.0	Paleosol
DB081	32.592220	-84.635800	162.5	Paleosol
DB082	32.500710	-84.945780	88.4	Paleosol
DB083	32.500810	-84.945490	87.5	Paleosol
DB084	32.580580	-84.930020	184.1	Metamorphic
DB085	32.571510	-84.929850	167.6	Metamorphic
DB086	32.523670	-84.868650	116.4	Paleosol
DB087	32.518420	-84.842960	109.4	Paleosol
DB088	32.518750	-84.843330	112.2	Paleosol
DB089	32.525840	-84.839010	124.7	Paleosol
DB090	32.527690	-84.844080	107.0	Paleosol
DB091	32.530170	-84.843090	118.6	Paleosol
DB092	32.551620	-84.818250	135.9	Paleosol
DB093	32.554550	-84.814630	143.6	Paleosol
DB094	32.554580	-84.813990	135.9	Metamorphic
DB095	32.554660	-84.814580	143.6	Tuscaloosa sand
DB096	32.555700	-84.815010	136.2	Metamorphic
DB097	32.547550	-84.811660	134.4	Paleosol
DB098	32.547000	-84.812050	137.8	Paleosol
DB099	32.493280	-84.921090	80.8	Bed of Cooper Creek adjacent to Parkhill Cemetery
DB100	32.462040	-84.998740	58.8	Sandstone in contact w/ basement (Paleosol may be present)
DB101	32.460620	-84.999550	79.2	Tuscaloosa
DB102	32.482650	-85.033200	120.1	Tuscaloosa sand near Phenix City Kmart
DB103	32.552680	-84.867050	136.9	Bedrock in place along Fall Line Trace
DB104	32.552730	-84.866900	136.9	Possibly Tuscaloosa

Appendix D: Station Number, Latitude, Longitude, Elevation and Lithologic Data for Stations on the Coastal Plain Unconformity.

Name	Station ID	Latitude	Longitude	Elev (m)	Description
CPUA001	FT079	32.542800	-84.945000	126.2	Metamorphic rock immediately below Tuscaloosa
CPUA002	FT096	32.521800	-84.956900	128.6	Possible Tuscaloosa above gneiss
CPUA003	FT097	32.582600	-84.910900	186.5	Metamorphic rock immediately below Tuscaloosa
CPUA004	FT030	32.539500	-84.933300	117.3	Igneous below Tuscaloosa
CPUA005	FT056	32.534274	-84.981800	114.9	Tuscaloosa above gneiss (CP unconformity)
CPUA006	FT076	32.523531	-84.948898	140.2	Tuscaloosa just above basement
CPUA007	FT096	32.521800	-84.956900	128.9	Probable Tuscaloosa above gneiss
CPUA008	F&H, 1987	32.551725	-84.684896	140.2	Tuscaloosa above gneiss (CP unconformity)
CPUA009	STC007	32.539648	-84.898961	127.4	Tuscaloosa sand immediately above gneiss (paleovalley CP unconformity)
CPUA010	M&F, 1975	32.506795	-84.964115	107.0	Tuscaloosa immediately above weathered gneiss (CP unconformity)
CPUA011	DB074	32.554890	-84.8756	141.1	Contact
CPUA012	DB099	32.49328	-84.92109	80.8	Bed of Cooper Creek adj to Parkhill Cemetery
CPUA013	DB100	32.462040	-84.99874	58.8	Sandstone in contact w/ basement (Paleosol may be present)

400

Appendix E: Interpolated Stations on the Coastal Plain Unconformity.

Name	Latitude (N)	Longitude	Elev (m)	Basement Station ID	Latitude	Longitude	Elev (m)	Sed Station ID	Latitude	Longitude	Elev (m)	Distance (m)	Elev Diff (m)
CPUB001	32.541662	-84.896586	142.8	1992112703	32.541343	-84.897141	142.6	STC008	32.541980	-84.896030	143.0	126	0.3
CPUB002	32.541667	-84.897222	141.6	1992112701	32.541189	-84.898530	140.2	STC008	32.541980	-84.896030	143.0	250	2.7
CPUB003	32.542222	-84.895833	143.1	FT088	32.542400	-84.895600	143.3	STC008	32.541980	-84.896030	143.0	62	0.3
CPUB004	32.520278	-84.986944	125.9	1980092601	32.520378	-84.987846	124.4	FT004	32.520400	-84.986000	127.4	173	3.0
CPUB005	32.520833	-84.987222	126.9	09032502	32.521150	-84.988633	126.5	FT004	32.520400	-84.986000	127.4	261	0.9
CPUB006	32.521389	-84.985000	132.6	1982042201	32.522171	-84.983744	137.8	FT004	32.520400	-84.986000	127.4	289	10.4
CPUB007	32.547222	-84.927500	149.2	1980062201	32.546085	-84.928163	146.0	DB010	32.548280	-84.926960	152.4	269	6.4
CPUB008	32.560833	-84.590000	132.4	DB062	32.560960	-84.590200	131.1	DB061	32.560730	-84.589740	133.8	50	2.7
CPUB009	32.505000	-84.938611	117.8	STC003	32.505219	-84.939033	114.9	STC004	32.504524	-84.938194	120.7	110	5.8
CPUB010	32.512222	-84.922500	109.1	STC005	32.511920	-84.922620	109.7	FT015	32.512400	-84.922500	108.5	55	1.2
CPUB011	32.542778	-84.805556	123.4	DB027	32.542370	-84.806240	124.7	DB029	32.543060	-84.805100	122.2	132	2.4
CPUB012	32.564167	-84.641111	150.0	DB051	32.564410	-84.639720	146.9	DB050	32.563810	-84.642680	153.0	285	6.1
CPUB013	32.545556	-84.643333	129.2	DB042	32.545280	-84.644160	127.1	DB043	32.545920	-84.642560	131.4	166	4.3
CPUB014	32.547778	-84.810278	132.9	DB097	32.547550	-84.811660	134.4	DB024	32.547830	-84.808680	131.4	281	3.0
CPUC001	32.520278	-84.987778	123.9	1980050104	32.520241	-84.989308	120.4	FT004	32.520400	-84.986000	127.4	311	7.0
CPUC002	32.521667	-84.985000	131.8	1982042202	32.522812	-84.983915	136.2	FT004	32.520400	-84.986000	127.4	332	8.8
CPUC003	32.521389	-84.987778	123.1	1980102903	32.522620	-84.989607	118.9	FT004	32.520400	-84.986000	127.4	419	8.5
CPUC004	32.549722	-84.893611	147.8	08071303	32.551217	-84.926850	143.3	DB010	32.548280	-84.926960	152.4	327	9.1
CPUC005	32.549722	-84.926667	148.7	1981050501	32.551263	-84.926600	145.1	DB010	32.548280	-84.926960	152.4	333	7.3
CPUC006	32.505833	-84.940000	108.4	FT046	32.506900	-84.941700	96.0	STC004	32.504524	-84.938194	120.7	422	24.7
CPUC007	32.506389	-84.938056	109.7	07030201	32.508367	-84.937967	98.8	STC004	32.504524	-84.938194	120.7	428	21.9
CPUC008	32.550556	-84.873056	136.1	FT089	32.552200	-84.873800	134.7	FT067	32.548700	-84.872300	137.5	414	2.7
CPUC009	32.557778	-84.841389	152.4	1980080703	32.558563	-84.842807	152.7	DB064	32.557080	-84.840030	152.1	308	0.6
CPUC010	32.558333	-84.841389	148.7	07022401	32.559417	-84.842867	145.4	DB064	32.557080	-84.840030	152.1	372	6.7
CPUC011	32.548056	-84.811111	126.5	DB067	32.548440	-84.813480	118.6	DB024	32.547830	-84.808680	134.4	455	15.8
CPUC012	32.551667	-84.766389	132.7	1990101701	32.550857	-84.764574	124.4	DB030	32.552730	-84.768150	141.1	395	16.8
CPUC013	32.594167	-84.636944	167.6	DB080	32.592150	-84.637210	167.0	DB048	32.596170	-84.636590	168.2	451	1.2
CPUC014	32.594167	-84.636111	165.4	DB081	32.592220	-84.635800	162.5	DB048	32.596170	-84.636590	168.2	445	5.8

Name	Latitude (N)	Longitude	Elev (m)	Basement Station ID	Latitude (N)	Longitude	Elev (m)	Sed Station ID	Latitude	Longitude	Elev (m)	Distance (m)	Elev Diff (m)
CPUC015	32.547500	-84.810278	134.6	DB098	32.547000	-84.812050	137.8	DB024	32.547830	-84.808680	131.4	329	6.4
CPUD001	32.521389	-84.988611	116.7	1981060702	32.522585	-84.991326	106.1	FT004	32.520400	-84.986000	127.4	555	21.3
CPUD002	32.521667	-84.988611	115.4	09032501	32.522983	-84.991100	103.3	FT004	32.520400	-84.986000	127.4	558	24.1
CPUD003	32.520278	-84.988889	116.3	1981060705	32.520029	-84.992040	105.2	FT004	32.520400	-84.986000	127.4	568	22.3
CPUD004	32.540278	-84.981944	141.0	1978100501	32.542225	-84.984023	139.6	FT055	32.538300	-84.979700	142.3	596	2.7
CPUD005	32.548056	-84.923889	137.6	1980050503	32.547977	-84.921077	122.8	DB010	32.548280	-84.926960	152.4	552	29.6
CPUD006	32.550556	-84.926944	151.0	FT068	32.552600	-84.926700	149.7	DB010	32.548280	-84.926960	152.4	481	2.7
CPUD007	32.504167	-84.941111	104.5	STC001	32.503536	-84.944123	88.4	STC004	32.504524	-84.938194	120.7	567	32.3
CPUD008	32.505556	-84.941111	108.1	FT047	32.506400	-84.944200	95.4	STC004	32.504524	-84.938194	120.7	601	25.3
CPUD009	32.506944	-84.937222	110.9	1978120601	32.509173	-84.936070	101.2	STC004	32.504524	-84.938194	120.7	554	19.5
CPUD010	32.509722	-84.922222	97.5	FT015	32.512400	-84.922500	107.9	FT025	32.507300	-84.921800	87.2	571	20.7
CPUD011	32.546667	-84.870278	132.3	07030401	32.544483	-84.868417	127.1	FT067	32.548700	-84.872300	137.5	594	10.4
CPUD012	32.548333	-84.811667	127.4	DB065	32.548720	-84.814920	120.4	DB024	32.547830	-84.808680	134.4	593	14.0
CPUD013	32.548056	-84.811667	127.4	DB066	32.548210	-84.814920	120.4	DB024	32.547830	-84.808680	134.4	586	14.0
CPUD014	32.551667	-84.765833	132.7	1990101702	32.550478	-84.763554	124.4	DB030	32.552730	-84.768150	141.1	498	16.8
CPUD015	32.550833	-84.765833	131.5	1990101704	32.548825	-84.763771	121.9	DB030	32.552730	-84.768150	141.1	598	19.2
CPUD016	32.579722	-84.890556	170.7	FT092	32.581900	-84.891300	175.6	FT091	32.577700	-84.889900	165.8	485	9.8
CPUD017	32.565278	-84.636944	152.9	DB051	32.564410	-84.639720	146.9	DB049	32.566230	-84.634250	158.8	551	11.9
CPUD018	32.550000	-84.810278	126.6	09070805	32.552267	-84.811983	121.9	DB024	32.547830	-84.808680	131.4	583	9.4
CPUD019	32.538056	-84.814722	117.3	DB077	32.539340	-84.812910	110.0	DB079	32.536710	-84.816730	124.7	462	14.6
CPUD020	32.521111	-84.915278	110.0	FT028	32.522100	-84.912300	104.2	FT027	32.520100	-84.918200	115.8	596	11.6

Sample DB039
 Initial Weight (g) 49.564
 Weight Retained (g) 49.272

Appendix F: Grain Size Analysis

Sample DB039
 Initial Weight (g) 49.564
 Weight Retained (g) 49.272

Φ	Weight Retained (g)	Individual %	Cumulative %
-2.0	0.315	0.6	0.315
-1.5	0.405	0.8	1.1
-1.0	0.633	1.3	2.4
-0.5	3.406	6.9	9.3
0	6.573	13.3	22.5
0.5	9.260	18.7	41.2
1.0	10.072	20.3	61.5
1.5	8.586	17.3	78.9
2.0	4.180	8.4	87.3
2.5	1.964	4.0	91.3
3.0	1.390	2.8	94.1
3.5	0.971	2.0	96.0
4.0	0.524	1.1	97.1
>4.0	0.993	2.0	99.1

Sample DB043
 Initial Weight (g) 49.733
 Weight Retained (g) 49.489

Φ	Weight Retained (g)	Individual %	Cumulative %
-2.0	0.094	0.2	0.094
-1.5	1.207	2.4	2.5
-1.0	4.508	9.1	11.6
-0.5	8.948	18.0	29.6
0	9.776	19.7	49.2
0.5	8.124	16.3	65.6
1.0	6.786	13.6	79.2
1.5	4.519	9.1	88.3
2.0	2.724	5.5	93.8
2.5	1.186	2.4	96.2
3.0	0.721	1.4	97.6
3.5	0.389	0.8	98.4
4.0	0.157	0.3	98.7
>4.0	0.350	0.7	99.4

Sample DB088
Initial Weight (g) 49.383
Weight Retained (g) 49.917

Φ	Weight Retained (g)	Individual %	Cumulative %
-2.0	0	0.0	0
-1.5	0.071	0.1	0.1
-1.0	0.51	1.0	1.2
-0.5	4.165	8.4	9.6
0	5.022	10.2	19.8
0.5	6.552	13.3	33.0
1.0	9.684	19.6	52.7
1.5	10.313	20.9	73.5
2.0	6.122	12.4	85.9
2.5	2.153	4.4	90.3
3.0	1.692	3.4	93.7
3.5	1.368	2.8	96.5
4.0	0.635	1.3	97.8
>4.0	0.630	1.3	99.1

Sample DB100
Initial Weight (g) 49.695
Weight Retained (g) 49.364

Φ	Weight Retained (g)	Individual %	Cumulative %
-2.0	2.22	4.5	4.5
-1.5	3.594	7.2	11.7
-1.0	4.149	8.3	20.0
-0.5	5.276	10.6	30.7
0	5.925	11.9	42.6
0.5	6.428	12.9	55.5
1.0	5.293	10.7	66.2
1.5	4.756	9.6	75.7
2.0	4.059	8.2	83.9
2.5	2.632	5.3	89.2
3.0	2.253	4.5	93.7
3.5	1.311	2.6	96.4
4.0	0.545	1.1	97.5
>4.0	0.923	1.9	99.3

Sample DB102 Lower
Initial Weight (g) 49.633
Weight Retained (g) 49.120

Φ	Weight Retained (g)	Individual %	Cumulative %
-2.0	0.415	0.8	0.8
-1.5	2.561	5.2	6.0
-1.0	9.15	18.4	24.4
-0.5	7.462	15.0	39.5
0	6.599	13.3	52.8
0.5	6.438	13.0	65.7
1.0	5.953	12.0	77.7
1.5	5.318	10.7	88.4
2.0	3.030	6.1	94.5
2.5	0.982	2.0	96.5
3.0	0.523	1.1	97.6
3.5	0.312	0.6	98.2
4.0	0.105	0.2	98.4
>4.0	0.272	0.5	99.0

Sample DB102 Middle
Initial Weight (g) 49.607
Weight Retained (g) 49.307

Φ	Weight Retained (g)	Individual %	Cumulative %
-2.0	0.152	0.3	0.3
-1.5	0.341	0.7	1.0
-1.0	0.795	1.6	2.6
-0.5	3.190	6.4	9.0
0	6.092	12.3	21.3
0.5	12.347	24.9	46.2
1.0	12.096	24.4	70.6
1.5	6.941	14.0	84.6
2.0	3.463	7.0	91.6
2.5	1.377	2.8	94.3
3.0	0.870	1.8	96.1
3.5	0.567	1.1	97.2
4.0	0.249	0.5	97.7
>4.0	0.827	1.7	99.4

A POTENTIAL LONG-LIVED UPPER CRETACEOUS PALEODRAINAGE SYSTEM IN
THE U.S. SOUTHWESTERN GEORGIA-SOUTHEASTERN ALABAMA REGION

A thesis submitted to the College of Letters and Science in partial fulfillment of the requirements
for the degree of

MASTER OF SCIENCE
DEPARTMENT OF EARTH AND SPACE SCIENCE

by

Daniel L. Black

2015

Dr. Clinton Barineau, Chair

Dr. William Frazier, Member

Dr. Roger Brown, Member

Date

Dr. William Frazier, Department Chair

